2019

Effect of Endothelial Progenitor Cell-derived Exosomes on High Glucose and Hypoxia/ Reoxygenation-induced Injury of Astrocytes

Manasi Suchit Halurkar
Wright State University

EFFECT OF ENDOTHELIAL PROGENITOR CELL-DERIVED EXOSOMES ON HIGH GLUCOSE AND HYPOXIA/REOXYGENATION-INDUCED INJURY OF ASTROCYTES

A thesis submitted in partial fulfilment of the
requirements for the degree of
Master of Science

by

MANASI SUCHIT HALURKAR

B. Pharm, University of Mumbai, India, 2015

2019

Wright State University

WRIGHT STATE UNIVERSITY

GRADUATE SCHOOL

1st JULY 2019

I HEREBY RECOMMEND THAT THE THESIS PREPARED UNDER MY SUPERVISION BY Manasi Suchit Halurkar ENTITLED, Effect of endothelial progenitor cell-derived exosomes on high glucose and hypoxia/reoxygenation-induced injury of astrocytes. BE ACCEPTED IN PARTIAL FULFILLMENT OF THE REQUIREMENTS FOR THE DEGREE OF Master of Science.

Ji C. Bihl, M.D., Ph.D.
Thesis Director

Jeffrey B. Travers, M.D., Ph.D.
Chair, Department of
Pharmacology and Toxicology

Committee on Final Examination

Ji C. Bihl, M.D., Ph.D.

Yanfang Chen, M.D., Ph.D.

Adrian Corbett, Ph.D.

Barry Milligan, Ph.D.
Interim Dean of the Graduate School

ABSTRACT

Halurkar, Manasi Suchit. M.S. Department of Pharmacology and Toxicology, Wright State University, 2019. Effect of endothelial progenitor cell-derived exosomes on high glucose and hypoxia/reoxygenation-induced injury of astrocytes.

In this study, we tested the protective effects of EPC-EXs (endothelial progenitor cell derived exosomes) and miR-126 EPC-EXs (microRNA-126 EPC-EXs) on the astrocytes injured by HG (high glucose) plus H/R (hypoxia/reoxygenation) model. At first, we determined the concentration and time dependent uptake of EPC-EXs by astrocytes. It was also found that the EPC-EXs were uptaken via macropinocytosis, caveolin-dependent and clathrin-mediated pathways in astrocytes. Furthermore, the astrocyte cell line was injured through the HG + H/R model. EXs, isolated by ultracentrifugation from the EPC culture supernatant were co-incubated with the injured cells. It was found that EPC-EXs and miR-126 EPC-EXs decrease apoptosis, lipid peroxidation, oxidative stress and cytotoxicity in the injured cells, hence protecting them.

Table of Contents

List of Figures

List of Tables

ACKNOWLEDGMENTS

I would first like to thank my Advisor Dr. Ji C. Bihl, for her constant support, motivation and intellectual direction for the past two years of my time in her laboratory. Dr. Bihl is an inspiration with her dedication towards the research and amazing project ideas. She has been a great guide throughout the period and always been there for support with the knowledge gaps when required. I am very privileged to have had the opportunity to work in her laboratory under her mentorship and would look forward to somehow be a part of her research as the time passes. Without her guidance, this project would not have been completed.

I would like to extend my thanks to Dr. Yanfang Chen and Dr. Adrian Corbett for serving on my thesis committee. Their valuable comments and directions through our meetings allowed me to understand the loopholes and work on them effectively.

I would also like to thank Dr. Bihl's lab members Dr. Jinju Wang, Dr. Shuzhen Chen, Yuchen Li (Jasson) for their unparalleled assistance and guidance for the research work. They taught me how to conduct the experiments, from the scratch and kept immense patience all along.

I am grateful to the Department of Pharmacology and Toxicology for providing me with the excellent coursework which was also helpful as a part of my research, along with the great teachings provided by all the Professors for my master's program.

Finally, I would like to extend my thanks to my family and friends, without whose encouragement, support and motivation, nothing of this could be possible.

I. INTRODUCTION

1. Ischemic Stroke

1.1. Prevalence, definition and types

The third leading cause of death in the United States is stroke, killing around 140,000 people each year [1]. It leads to long-term serious disability, high frequency of recurrence, reduction in mobility and other unfortunate consequences [2]. Stroke is a cerebrovascular accident, also known as a brain attack, is defined as a global or acute neurological deficit that is bound to last for more than 24 hours or leading to death [4]. It occurs when the blood supply to the brain is interrupted unexpectedly, leading to the death of the brain cells which are bereft of the nutrition and oxygen supplied by the blood [3]. It is broadly classified, on the basis of its underlying pathological condition, into ischemic stroke and haemorrhagic stroke and has no etiology other than the vascular origin. Ischemic stroke occurs when blood vessel carrying blood to the brain is obstructed via a thrombus formation within or an embolus, while the rupture of a blood vessel leads to haemorrhagic stroke [5]. However, an acute stage of stroke which is known as the Transient Ischemic Attack (TIA) is defined as a temporary event wherein the signs and symptoms of stroke resolve within 24 hours of its occurrence [6].

Ischemic stroke accounts for 80% of the total stroke cases and is more prevalent with growing age and changing lifestyle of people. It occurs when a cerebral artery, an artery carrying blood to the brain, is blocked thus the blood supply is interrupted, resulting in

death of the brain cells due to lack of sufficient oxygen and nutrition [3]. The block could either be a result of a thrombus formation, which can be a fat-based plaque or a blood clot, within the blood vessel leading to thrombotic ischemic stroke or an embolus, which is a free-formed clot formed elsewhere in the circulation but lodges itself into the cerebral blood vessel thus leading to embolic ischemic stroke [7]. It can also be a result of stenosis wherein the blood vessel narrows due to the fat deposition and clots along the vessel walls [8].

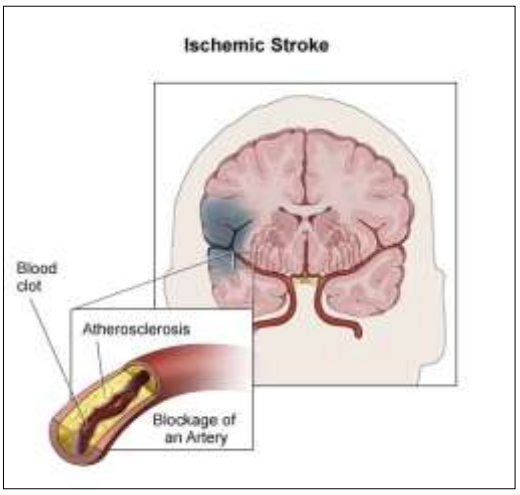

*Fig 1:***Ischemic Stroke.** The atherosclerotic blood clot within the cerebral blood vessel leading to hypoxic condition in the brain thus cell death [9].

1.2. Risk factors

There are various underlying causes and risk factors associated with ischemic stroke. These factors can be classified into modifiable and non-modifiable factors. The non-modifiable risk factors, which tend to be the markers for higher risk of stroke, include age, sex, race-ethnicity, heredity and geographical location. Incidence and risk of stroke occurrence increases with increasing age, wherein after 55 years of age it doubles for every decade.

Higher occurrence in women however more deaths due to stroke reported in men, a possible reason being that the women outlive the men. Higher stroke occurrences found in African Americans (2-4 folds), Hispanics (2 folds) and Chinese in comparison to non-Hispanic Whites. Higher incidence in first-degree relatives by 2 folds [10].

The modifiable risk factors on the other hand are the reversible aspects which account for the lower risk of stroke being amenable to intervention. These factors include various conditions and diseases such as hypertension, atrial fibrillation, coronary heart diseases, left ventricular hypertrophy, alcohol consumption, obesity, diabetes mellitus, smoking, hyperlipidaemia and physical inactivity [3,10, 11, 12]. These conditions are responsible for increased incidence of ischemic stroke and thus need to be taken care of medically in order to avoid the stroke risk.

Non-Modifiable	Modifiable
Age	Hypertension
Gender	Diabetes Mellitus
Race	Atrial Fibrillation
Ethnicity	Cardiac disease
Previous stroke history	Smoking
	Alcohol Consumption
	Oral contraceptives
	Hyperlipidaemia
	Transient Ischemic Attack
	Hormone therapy
	Physical inactivity

Table 1: **Risk factors associated with stroke.**

1.3. Diagnosis and treatment

A series of diagnostic procedures are available to determine stroke development as well as its location. Procedures such as computerized tomography (CT) scan gives a detailed image

of the brain focussing on the blood vessels in the neck and brain by the means of X-rays, magnetic resonance imaging (MRI) employ magnetic and radio waves to detect tissue

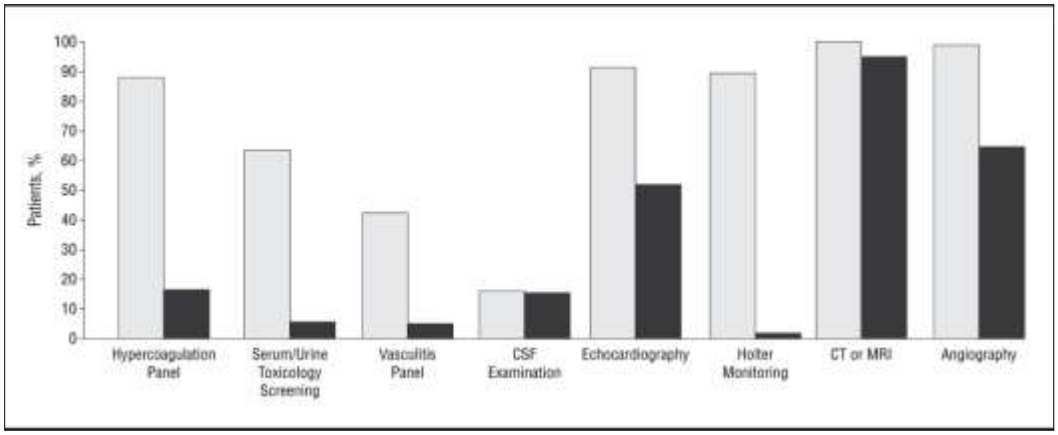

*Fig 2:***Diagnostic tests for ischemic stroke in young adults.** The figure is a graphical representation of percentage of patients who underwent a certain test and the percentage which depicted positive results for the same. CSF-Cerebrospinal fluid, CT-Computed Tomography, MRI-Magnetic resonance imaging [15].

damage in the brain, carotid ultrasound shows the build-up of plaque and blood clot by using sound waves and by cerebral angiogram wherein a dye is injected into a major blood vessel and then imaged using X-rays for any block or clot inside the vessel [13,14].

Ischemic stroke is an expensive as well as a life-threatening disease costing around $40 billion to the US economy every year [16]. The primary motive of a therapy for this disease is to either reverse or limit the complications, occurring after the onset, for the patient to recover. The most standard mode of treatment employed for ischemic stroke is the use of a thrombolytic agent, recombinant tissue plasminogen activator (rtPA) administered intravenously (IV). This is the only approved therapeutic agent by the Food and Drug Administration (FDA) for this disease condition till date. Although, only a few (3-5%) of the stroke sufferers receive this treatment on time [17]. tPA is a serine protease by nature which is converted into synthetic products by the means of recombinant technology thus naming it as rtPA. Being a thrombolytic, it dissolves the clot by breaking the fibrin

molecules through the plasmin which is released from the activated plasminogen which is fibrin-bound [18].

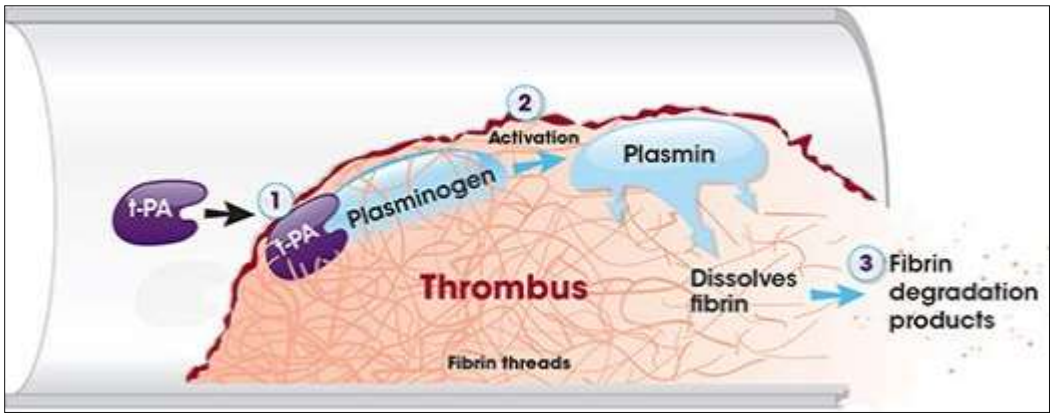

Fig 3: **Mechanism of action of rtPA.** rtPA binds to the fibrin mesh (formed by platelet aggregation resulting in clot formation) thus activating the fibrin-bound plasminogen complex. This activation leads to the release of plasmin from the complex which breaks up the clots by breaking up the fibrin molecules thus inititating the process of fibrinolysis [18,19,20].

However, the treatment with rtPA is only viable for a small percentage of patients due to a narrow therapeutic window of this drug, which lasts for upto 4.5 hours after the event onset. Other therapies include the treatment via stem cell therapy, using various biomaterials and mechanical thrombectomy as a part of endovascular intervention [21,22].

2. Diabetes Mellitus

2.1. Prevalence, definition and types

Diabetes mellitus, a chronic metabolic disorder associated with high blood glucose is one of the major leading causes of death in the United States, reported as 7th in year 2015. As per the guideline report presented by the International Diabetes Federation (IDF), the number of people suffering from diabetes mellitus has been growing ever since [23,24]. The prime risk factors associated with the occurrence of this disorder are age, history of diabetes, lifestyle, smoking, ethnic origin, obesity and improper diet. Although a higher

incidence of diabetes is observed in the population in the passing years, however around 30% of them are found to be undiagnosed cases. It is also a leading cause of various complications such as cardiovascular and kidney diseases, retinopathy, limb amputations and many such co-morbidities [25].

Diabetes mellitus is defined as a chronic disease or a metabolic syndrome wherein a rise in blood glucose levels observed as a result of ineffective production of insulin by the pancreas or the inability of body to respond to the insulin effectively. This increase in blood glucose levels is responsible for damaging various body systems namely the blood vessels and nerves [26]. Depending on its etiology, diabetes mellitus is classified into major two; Type I Diabetes Mellitus and Type II Diabetes Mellitus. Type I is also known as insulin-dependent diabetes while type II is often known as insulin-independent diabetes. However, there are other minorly classified types as well, such as gestational diabetes mellitus (GDM) and other specific types of diabetes [27,28].

2.2. Type I Diabetes Mellitus

Type I diabetes mellitus, also known as insulin-dependent diabetes which accounts 5-10% cases of diabetes, occurs due deficiency in insulin production thus leading to high blood glucose levels or hyperglycemia. This deficiency in insulin production is usually due to pancreatic β-cell destruction. It is broadly classified into immune-mediated diabetes and idiopathic diabetes. The patients suffering from type I diabetes need to be put on insulin therapy in order to maintain the normoglycemic (normal glucose) levels in the body [28,29].

2.3. Type II Diabetes Mellitus

This is the more common type of diabetes, found in about 90-95% of the diabetic population. Although more prevalent, it is the controllable and reversible type of disorder also known as insulin-independent diabetes [30]. In type II diabetes, the body develops insulin resistance wherein the cells do not respond to the signal by insulin to take up the blood sugar. Thus, leading to increased blood glucose levels as the glucose remains in the blood and not being used up by the cells. In the beginning when insulin resistance starts developing, it is known as the pre-diabetic phase which later on turns to complete resistance by all cells, leading to hyperglycemia and damage to other body systems eventually [31]. Obesity and physical inactivity are two of the few major causes of type II diabetes. This disorder is however reversible, in comparison to that of type I diabetes. It can be reversed by making changes to lifestyle, eating healthy, adequate exercise, intake of proper medication and quitting smoking and alcoholism. If left untreated or uncontrolled, it may lead to severe nerve damage, chronic kidney disease, stroke, wound healing problems, cardiovascular disorders, eye disease, lower extremities amputation, bladder problems and hindrance of sexual activity [32]. Type II diabetes mellitus is one of the leading causes for occurrence of ischemic stroke, thus patients with an underlying condition of diabetes are at higher risk for developing stroke.

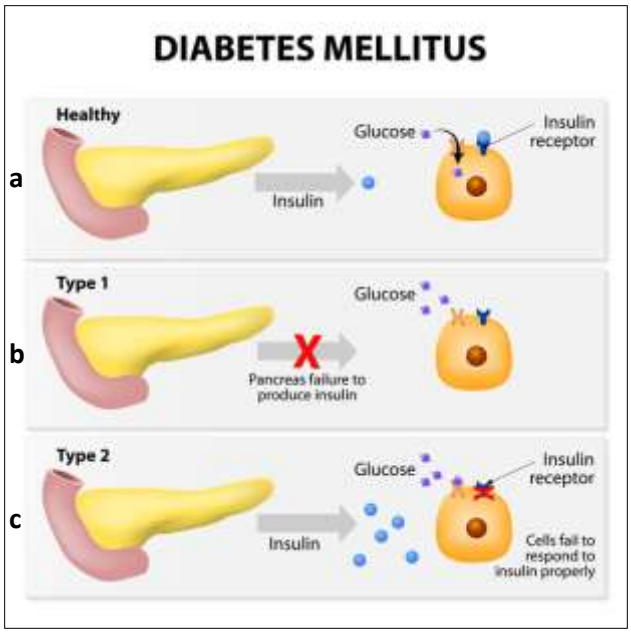

Fig 4: **Types of Diabetes Mellitus.** a) Healthy condition: Efficient uptake of the glucose circulating in blood by the cell in response to the action of insulin on insulin receptor; b) Type I diabetes mellitus: Inability of pancreas to produce sufficient insulin, thus high blood glucose levels; and c) Type II diabetes mellitus: Pancreas produce sufficient amount of insulin but the cells are unable to respond to it efficiently [33].

2.4. Gestational Diabetes Mellitus (GDM) and Other Specific Types

GDM generally develops in 2-5% of pregnant women where insulin resistance is observed during pregnancy, which did not occur previously. Due to this insulin resistant and hyperinsulinemia, pregnant women develop diabetes. Various factors responsible for this insulin resistance are insulinase enzyme production, growth hormone alteration, cortisol and human placental lactogen secretion along with the insulin imbalance due to estrogen and progesterone [34].

Other specific types of diabetes mellitus, also known as secondary diabetes, mainly occur due to infection, endocrinopathies, chemical/ drug-induced diabetes, exocrine pancreas

disease, genetic defects in β-cell function and insulin resistance and other genetic syndromes related to diabetes [35].

2.5. Developing stroke due to diabetes mellitus

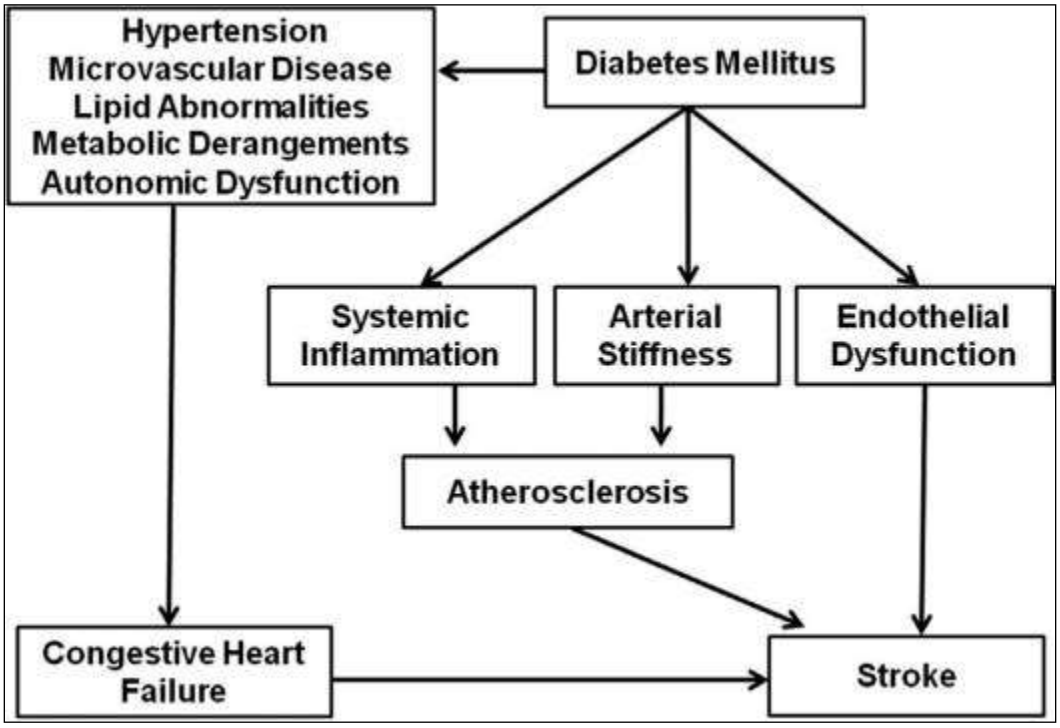

*Fig 5:***Possible mechanisms leading to stroke due to diabetes.** The various possible mechanisms leading to stroke due to the occurrence of diabetes mellitus within an individual [36].

Diabetes mellitus is one of the major modifiable risk factors for ischemic stroke. Individuals suffering from this syndrome are 1.5 times likely to be affected by stroke than the ones who are not [37]. The resulting hyperglycemia due to diabetes are responsible for causing fat deposits or blood clots within the blood vessels. Hyperglycaemic condition also leads to hardening of arterial walls and reduction in their elasticity thus leading to acceleration of atherosclerosis. Diabetes leads to impairment of Nitric Oxide (NO) mediated vasodilation due to increase in the inactivation of NO or because of decreased interaction between NO and the smooth muscles. This results in endothelial dysfunction which is one major cause of the resulting stroke in diabetic individuals [36]. Development

of atherosclerosis further leading to stroke is also a result of increased systemic inflammatory response predicted through the markers- adiponectin, C-reactive protein and cytokines (TNF-α, IL-1 & IL-6) [36, 38]. Thus, diabetes mellitus resulting into an ischemic stroke is at a higher risk because of these factors combined.

3. Endothelial Progenitor Cells (EPCs)

3.1. Origin and function

EPCs are referred to as the cell population which further mature into endothelial cells (ECs), thus known as the precursors of ECs. EPCs mobilize, differentiate and proliferate into mature ECs. Ashara et al. identified a hematopoietic population, which were CD34 and Flk1 positive mononuclear cells, having the potency to prompt vasculogenesis [39]. These are bone marrow-derived circulating cells originating in the blood of umbilical cord and periphery which were initially isolated using magnetic microbeads. These cells were termed to have the properties of embryonal angioblasts leading to neovascularization and re-endothelialisation. Apart from these functions, EPCs are involved in wound healing, angiogenesis, tissue regeneration as well as remodelling [40,41].

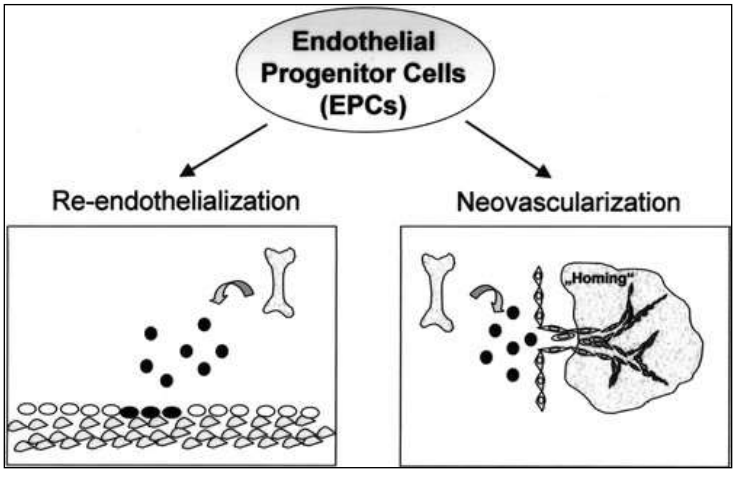

Fig 6: **Endothelial Progenitor Cell Function.** [42]

3.2. Role of EPCs in Ischemic Stroke

Previous studies involving EPCs have suggested that EPCs play a major therapeutic role in ischemic stroke.

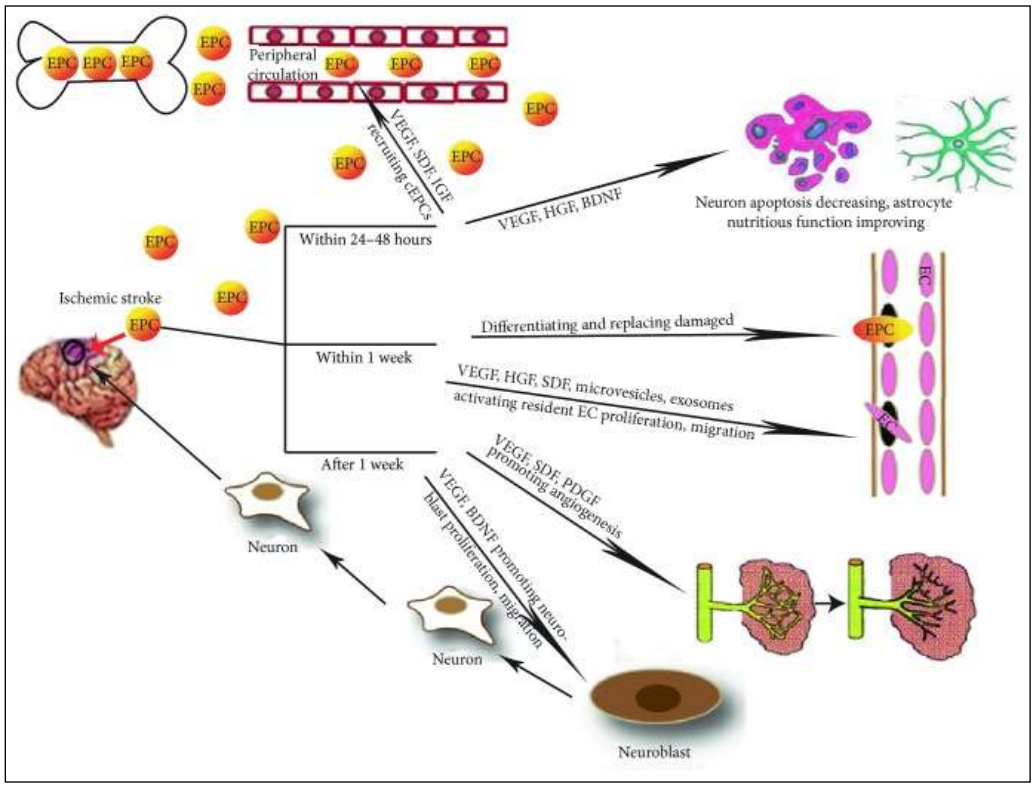

Fig 7: **Various roles of EPCs in treating stroke.** [43]

4. Exosomes

4.1. Introduction to exosomes

Exosomes are 30-100 nm sized, phospholipid bilayer extracellular vesicles (EVs). These vesicles, discovered around 30 years back, are formed within the cell and released in the extracellular space by undergoing a series of steps. Exosomes are released in the extracellular space by almost all cells, under normal physiological or stressful conditions and are found in biological fluids such as blood, urine, saliva, CSF and semen [44].

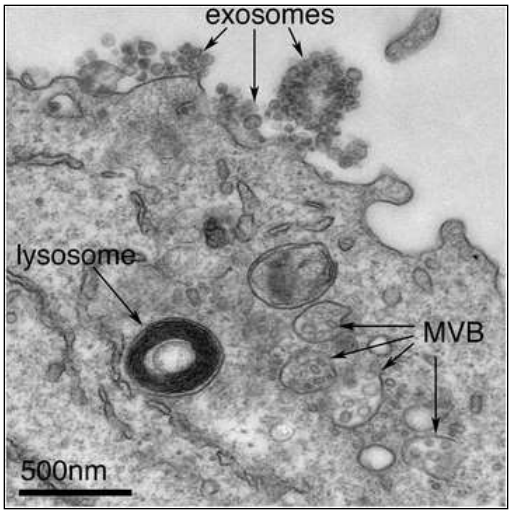

Fig 8: **Exosomes.** EXs released by Epstein–Barr virus-transformed B cell under Transmission Electron Microscopy [45].

At the time of initial discovery, these vesicles were thought to be cell debris, which were responsible for disposal of unwanted cellular components from the cellular environment. However, in recent years they have gained recognition in being responsible for intercellular communication, carrying information from one cell to another [46].

4.2. Biogenesis and Composition

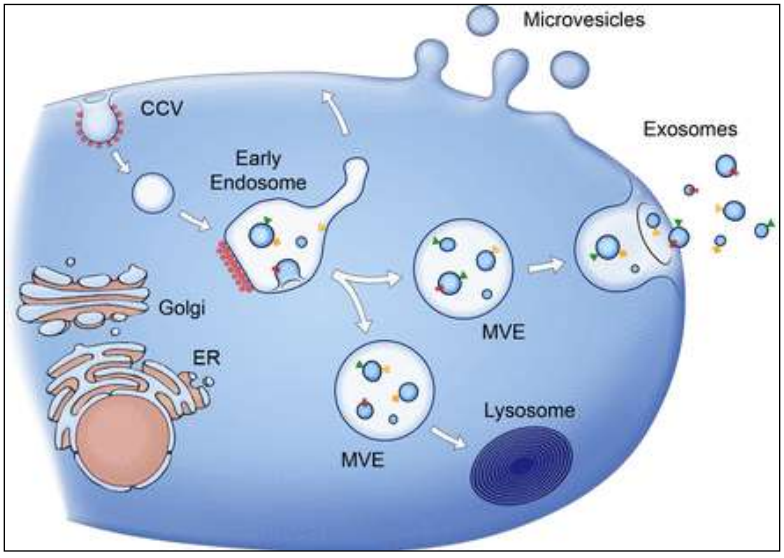

Fig 9: **Exosome biogenesis.** A brief insight into the EX biogenesis within a cell and their release in the extracellular space [47].

EXs generate within the early endosomes which are formed by inward budding of the plasma membrane. Early endosomes then mature into late endosomes also known as multivesicular endosomes (MVEs) containing the intraluminal vesicles (ILVs). The MVEs then fuse with the plasma membrane releasing the contents, which is the ILVs, into the extracellular space, then denoted as EXs [47, 48].

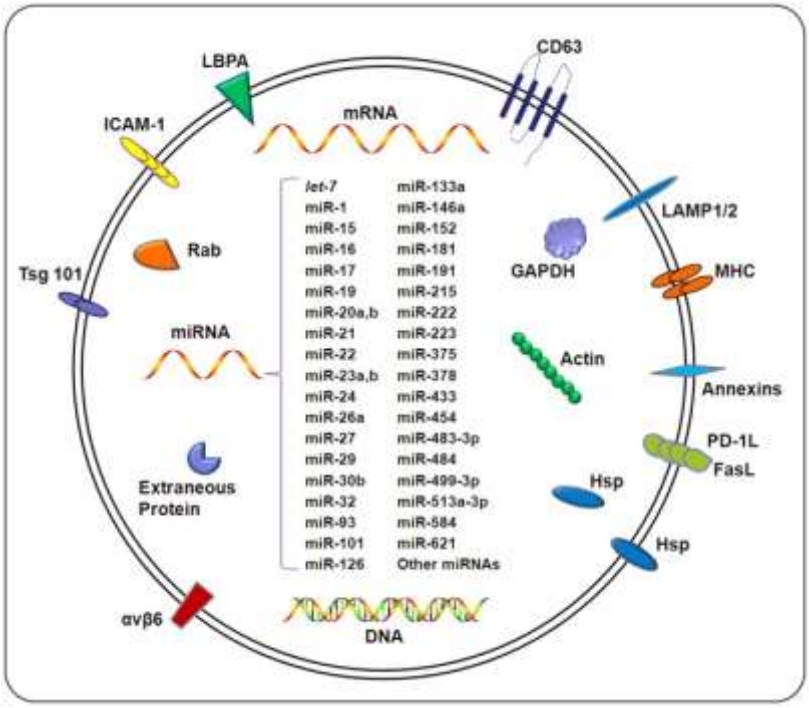

*Fig 10:***EX composition**. EXs are composed of a varied collection of biomolecules such as the mRNA, miRNA, DNA, proteins and lipids [49].

During the endosomal maturation stage, after which the MVEs are generated, cargo sorting within the endosomes occurs. Cargo sorting is responsible for the overall contents of the exosomes and hence their varied functions. This process is regulated by either Endosomal Sorting Complex Required for Transport (ESCRT)-mediated pathway or ceramide-dependent pathway. They are interchangeably known as non-ceramide pathway and non-ESCRT dependent pathway respectively. The ESCRT-mediated pathway incorporates four components, namely ESCRT-0, I, II and III, each of which are responsible for varied

functions in regard to the cargo sorting. While the ceramide-dependent pathway involves lipid rafts which are glycolipoprotein microdomains. However, the cargo carried by these EXs is a function of the parent cells within which these EXs are formed. The EXs are found to mainly contain mRNA, miRNA, DNA, lipids and proteins [48, 49, 50].

4.3. Isolation

There are various methods of EX isolation discovered over the years, and each of these methods have their own advantages and disadvantages on being looked for. Some of these methods are differential centrifugation (more commonly known as ultracentrifugation), density gradient centrifugation, filtration, size exclusion chromatography, polymer-based precipitation, sieving and immunological separation. The most commonly and widely used method, also known as the gold standard method of EX isolation, is the isolation by ultracentrifugation. Ultracentrifugation involves centrifugation at high-speed in order to obtain the EX pellet. It is the most commonly used method to derive EXs from biological fluids [51].

4.4. Detection and Characterization

EXs, after isolation, can be analysed by various methods for determining their morphology, quality, size and concentration. These methods are broadly classified into antibody-based, optical and biophysical methods. Various EX specific antibodies and arrays are available which are detected by FACS/flow cytometry or ELISA. The optical methods comprise of Nanosight Tracking analysis (NTA) which works by the principle of detection of Brownian motion of these particles under the laser; scattering flow cytometry (SFC), fluorescence microscopy and dynamic light scattering (DLS). While the biophysical methods involve

scanning electron microscopy (SEM), transmission electron microscopy (TEM) and atomic force microscopy (AFM) [52,53].

4.5. EX uptake

Literature and studies have suggested that there is more than one pathway or mechanism for the uptake of EXs by the cells. However, this uptake is a characteristic of the recipient cell rather than the donor cell. In the recent years, more studies are being conducted to know more about the uptake pathways and their unique characteristics. The uptake pathways are broadly classified into membrane fusion and endocytosis. Major uptake is carried out via the endocytic mechanism. Endocytosis is further classified into phagocytosis, macropinocytosis, clathrin-mediated endocytosis, caveolin-mediated endocytosis, lipid-raft mediated endocytosis and receptor mediated endocytosis (67).

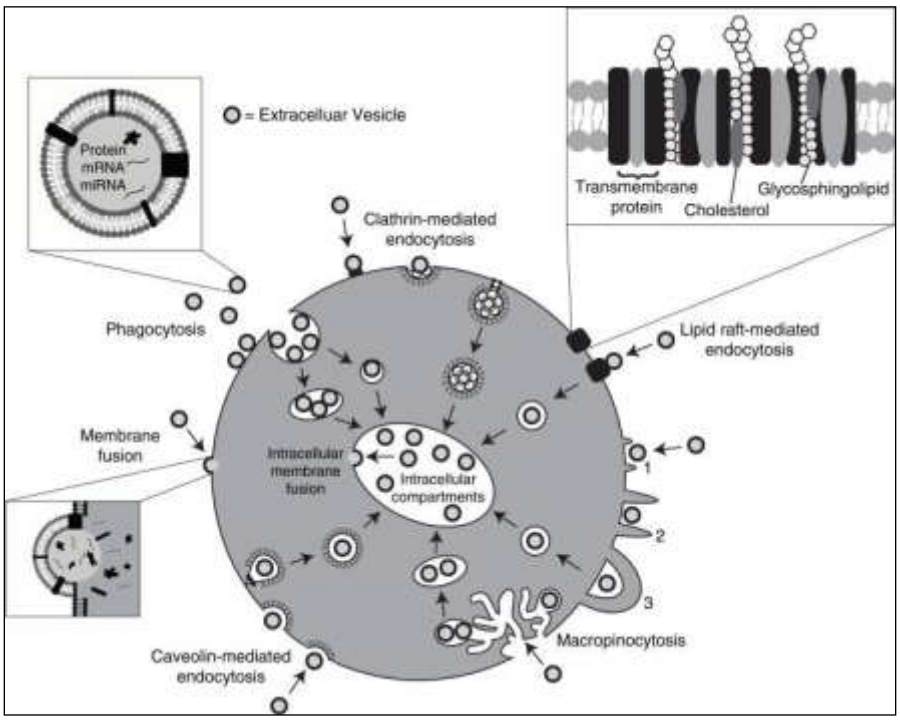

*Fig 11:***Pathways participating in EX uptake. [**67]

4.6. Function

Studies have suggested that EXs are involved in cellular signalling, wherein they carry information in the form of biomolecules from the parent cell to the recipient cell. This remains to be the unique function of EXs. Along with this, they are involved in facilitation of immune response, angiogenesis, wound healing, inflammation and coagulation [54]. They are also considered to be biomarkers in diagnosis and prognosis of various medical conditions and have proved to have immense diagnostic potential over the years. However, the most important property of EXs, which has gained some limelight over time, is that they can act as therapeutic agents and drug delivery carriers. The reason being the cargo present in these vesicles which is then expelled into the recipient cell for its own benefits. This cargo can then provide the required therapy. Although, the cargo either depends on the parent cell or if it has been edited for specific drug delivery [55].

4.7. Studies on EPC-EXs

Various studies in the recent years have focussed on the therapeutic efficacy of EPC-EXs. In year 2016, Li X. et al. determined that EPC-EXs are involved in vascular repair attenuation and acceleration of reendothelialization [56]. While, Li X. et al. and Zhang J. et al. proved that EPC-EXs accelerate cutaneous wound healing by promoting endothelial function and promoting angiogenesis via Erk1/2 signalling respectively [57, 58]. In 2017, Ke X. et al. found EPC-EXs responsible in increasing angiogenesis and proliferation in cardiac fibroblasts [59]. While Jia Y. et al. in 2019 suggested that EPC-EXs are involved in accelerating bone regeneration by regulating angiogenesis, in the distraction osteogenesis phase [60].

5. MicroRNA-126

5.1. Definition and Location

MicroRNA-126 (miR-126) is an endothelial-specific miRNA found to be expressed in a broad range of tissues, specifically the vascular system and highly vascularized tissues such as lungs and heart.

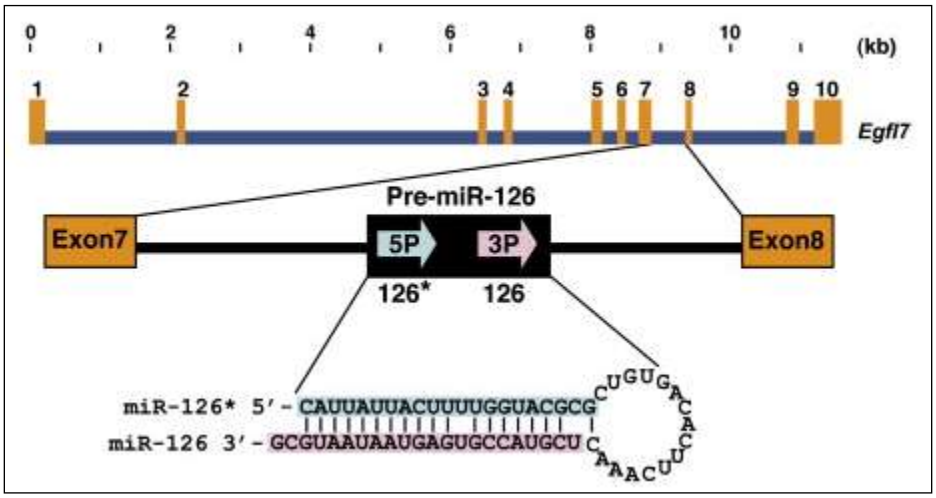

*Fig 12:***miR-126 location.** miR-126 located on chromosome 9 [61].

miR-126 is found on the human chromosome 9, located on the 7th intron of the epidermal growth factor-like domain 7 (EGFL7) gene. miR-126 is expressed in its stem loop structure with its complementary strand miR-126* [61].

5.2. Downstream Targets

Potential targets of miR-126 are vascular endothelial growth factor A (VEGF-A), vascular cell adhesion molecule 1 (VCAM-1), insulin receptor substrate 1 (IRS-1), sprouty related EVH1 domain containing 1 (SPRED-1) and PI3K (phosphoinositol-2-kinase) regulatory subunit p85 beta (PIK3R2).

5.3. Function

Like all other miRNAs, miR-126 also has specific functions. As miR-126 is endothelial specific, its functions also rely on that property. Hence, miR-126 is predominantly involved in angiogenesis and thus a prospective target for regulation of vascular integrity and treating various vascular disorders [62,63]. Studies have proved that priming of this miRNA in EPCs have been beneficial in enhancing their therapeutic efficacy in ischemic cerebral impairment [64]. It also functions in suppressing tumor growth in colorectal cancer through CXCR4 targeting, while being involved in rescuing cardiomyocytes efferocytosis due to diabetes [65, 66]. Owing to their therapeutic potential, they are deemed to be beneficial in stroke and diabetes related therapies.

II. HYPOTHESIS AND SPECIFIC AIMS

Hypothesis:

EPC-EXs could be uptaken by astrocytes and have protective effects on HG and H/R-injured astrocytes.

Specific aims:

Aim 1) 1a: To determine EPC-EXs uptake pattern in astrocytes.

1b: To determine the uptake mechanisms of EPC-EXs in astrocytes.

Aim 2) To assess the protective effects of EPC-EXs on HG and H/R-injured astrocytes.

Aim 3) To determine if miR-126 EPC-EXs have enhanced protective effects on HG and H/R-injured astrocytes.

III. EXPERIMENTAL DESIGN

Design for Aim 1a:

EPCs were cultured and allowed to be 80% confluent followed by serum starvation for 48 hours. The culture medium was collected for EX isolation. The obtained EPC-EXs were fluorescent labelled with PKH26 and resuspended in astrocyte (ASC) medium. Concentration-dependent uptake of the labelled EPC-EXs was determined by dividing the EPC-EXs in 3 concentrations - 1×10^9 , 2×10^9 and 3×10^9 EX particles/ml, which were added to the ASCs for 24 hours after which the cells were stained with DAPI and fluorescent images were obtained. Time-based uptake was determined by adding the labelled EPC-EXs to the ASC culture wherein the fluorescent images and flow cytometry data was obtained at 0, 2, 4, 6, 8, 10, 12, 14, 16, 18, 20, 22 and 24 hours.

Design for Aim 1b:

EPCs were cultured and allowed to be 80% confluent followed by serum starvation for 48 hours. The culture medium was collected for EX isolation. The obtained EPC-EXs were fluorescent labelled with PKH67 and resuspended in astrocyte (ASC) medium. On the other hand, the ASCs were cultured and grown till 80% confluency followed by treatment with vehicle, 80 μM Dynasore, 10 μM Pitstop 2, 200 μM Genistein or 5 μM LY294002 for 30 minutes. The cells were then washed and the labelled EPC-EXs were added for 24 hours.

The mechanism of uptake was determined by obtaining fluorescent images and performing flow cytometry. ASCs at passages 4-10 and EPCs at passages 4-12 were used for this study.

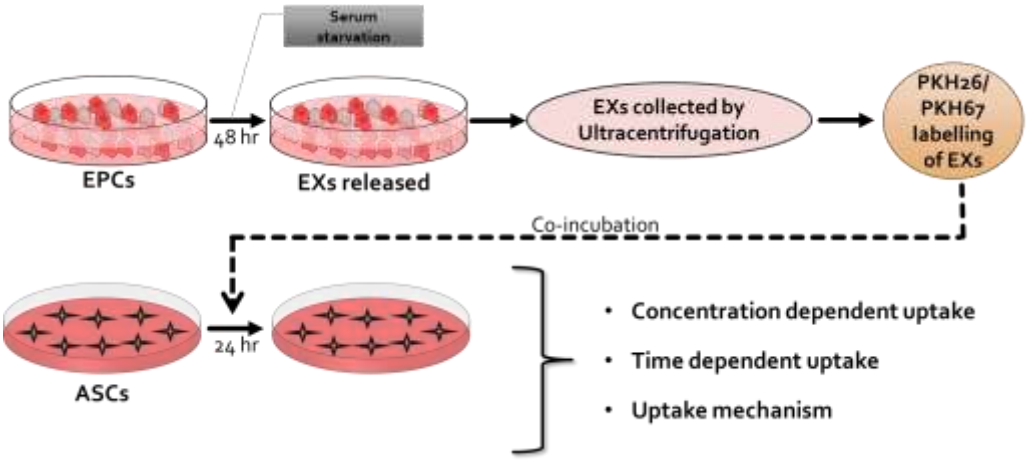

Fig 13: **Pictorial representation of Aim 1 experimental design.**

Design for Aim 2:

EPCs were cultured and allowed to be 80% confluent followed by serum starvation for 48 hours. The culture medium was collected for EX isolation and the obtained EPC-EXs were resuspended in ASC medium. ASCs were cultured and grown till 80% confluency, followed by subjecting to 25 mM glucose for 24 hours. After this these culture plates were put into the hypoxic chamber (with 1% O_2, 5% CO_2 and 94% N_2) for 6 hours, followed by reoxygenation for 24 hours. The isolated EPC-EXs were added to the cells during the reoxygenation phase for the 24 hour period after which apoptosis, oxidative stress, cytotoxicity and lipid peroxidation analysis were performed. ASCs at passages 4-10 and EPCs at passages 4-12 were used for this study.

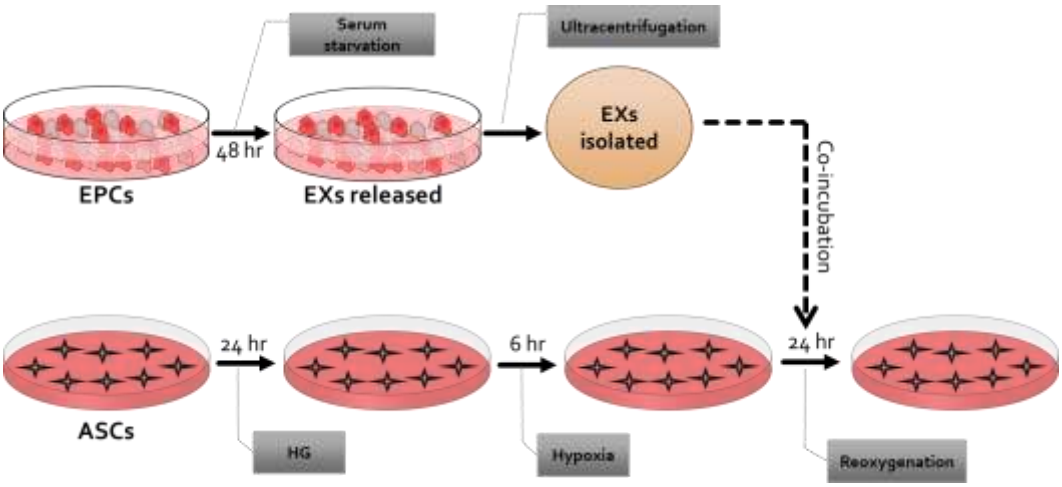

Fig 14: **Pictorial representation of Aim 2 experimental design.**

Design for Aim 3:

EPCs were cultured and allowed to be 70-80% confluent, after which they were transfected with miR-126 mimic using Dharmafect 1 transfection reagent, for 48 hours. Following the trasfection, the cells were serum starved for 48 hours for EX release. The medium was collected and miR-126 overexpressing EPC-EXs were isolated and resuspended in ASC medium. ASCs were cultured and grown till 80% confluency, followed by subjecting to 25 mM glucose for 24 hours. After this these culture plates were put into the hypoxic chamber (with 1% O_2, 5% CO_2 and 94% N_2) for 6 hours, followed by reoxygenation for 24 hours. The isolated EPC-EXs were added to the cells during the reoxygenation phase for the 24 hour period after which apoptosis, oxidative stress, cytotoxicity and lipid peroxidation analysis were performed. ASCs at passages 4-10 and EPCs at passages 4-12 were used for this study.

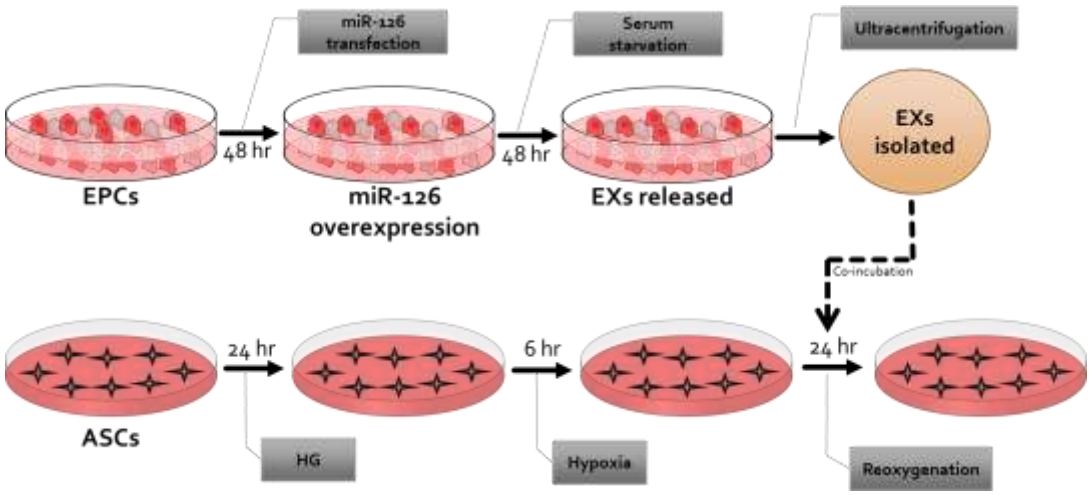

Fig 15: **Pictorial representation of Aim 3 experimental design.**

IV. MATERIALS AND METHODS

Materials

Human endothelial progenitor cells and human astrocytes were purchased from ATCC. Human endothelial progenitor cell culture expansion media serum free with antibiotics and human endothelial progenitor cell culture complete growth media with serum and antibiotics were purchased from Celprogen (Torrance, CA). Astrocyte medium was purchased from ScienCell (Carlsbad, CA). 0.05% trypsin-EDTA was purchased from Gibco. PKH26, PKH67 and Dynasore hydrate were purchased from Sigma-aldrich (St. Louis, MO). Dharmafect 1 from Dharmacon. miR-126 mimics were purchased from Applied biosystems. (D)-glucose and pierce LDH cytotoxicity kit were purchased from Fisher scientific. TRIzol reagent, dihydroethidium and Image-it lipid peroxidation kit were purchased from Invitrogen (Carlsbad, CA). Annexin V and propidium iodide (PI) were purchased from BDbiosciences. LY294002 was purchased from Enzo (Farmingdale, NY). Genistein was purchased from EMD Millipore (Israel). Pitstop 2 was purchased from Abcam (UK).

Cell culture

Human endothelial progenitor cells (HEPCs) and human astrocytes (ASCs) were used for this study. HEPCs were cultured in HEPC complete growth medium with serum and antibiotics in an incubator with standard cell culture conditions, that is 37°C and 5% CO_2. Culture medium was replaced every 2 days. EPCs at passages 4-12 were used for this study.

ASCs were cultured in ASC medium with 10% fetal bovine serum (FBS), 5% ASC growth factor and 5% penicillin/streptomycin (P/S) solution in a standard cell culture conditions maintaining incubator. Culture medium was replaced every 3 days. ASCs at passaged 4-10 were used for this study. For passaging both these cell types, with 85-90% cell confluence achieved, existing medium was replaced with 0.05% trypsin-EDTA at 37°C for 3 minutes, then the respective medium with serum was added to stop the reaction. This was centrifuged at 300 x g for 6 minutes, the pellet obtained was resuspended in respective culture medium and passaged in 1:3 ratio for further culture.

EX isolation

EPCs were cultured in serum-free medium for 48 hours. After serum starvation, culture medium was collected and centrifuged at 300 x g for 6 minutes, followed by 2000 x g for 20 minutes to remove the cells along with cell debris. The obtained supernatant was centrifuged at 20,000 x g for 70 minutes, this allowed the pelleting of microvesicles (MVs). As we do not make use of the MVs in our study, the obtained supernatant was subjected to ultracentrifugation at 170,000 x g for 90 minutes to pellet the EXs [69]. After ultracentrifugation, the supernatant was discarded, and the pellet was resuspended in 100 µl sterile-filtered phosphate buffer saline (PBS).

Nanoparticle tracking analysis (NTA)

The size and concentration determination of the isolated EPC-EXs was carried out by the instrument NS300 (Nanosight, Amesbury, UK). NTA visualizes and measures particle size and concentration by utilizing light scattering and Brownian motion properties. It can detect size distribution of particles in solution from 10 nm to 2 µm in diameter. The optimum particle concentration detected by NTA is ~10^7-10^9 particles/ ml. For better

detection, the EX samples were diluted with sterile-filtered PBS to a concentration of 10^7-10^8 particles / ml. After diluting the sample, 700 µl of the same was loaded in the instrument for movement tracking at the rate of 30 frames/ second. The videos with particle movement were recorded for at least 3 times per sample at different positions which were analysed by the NTA software (version 2.2, Nanosight). The NTA results were produced as a mean of the 3 tests performed per sample and the particle concentration was calculated after considering the accurate dilution factor for the NTA results.

EX labelling

To label the EXs, PKH26 or PKH67, lipophilic-membrane dyes exhibiting red or green fluorescence respectively, were used. The isolated EXs were added to a solution of 2 µl dye in 1 ml PBS for 5 minutes. In order to stop the reaction, 1ml 1% BSA was added and allowed to stand for a minute. This was then ultracentrifuged at 170,000 x g for 90 minutes, to obtain the fluorescent (PKH26 or PKH67) labelled EX pellet. The supernatant was discarded, and the pellet was resuspended in ASC medium for further co-incubation with the cells.

Injury model for ASCs

The experimental model for this study was that of high glucose (HG) plus hypoxia-reoxygenation (H/R) induced injury of ASCs, which is an in vitro representation of ischemic stroke due to diabetes mellitus. For inducing the HG + H/R injury, the ASCs were cultured in complete ASC medium until they were 80% confluent. Following this, the ASCs were subjected to 25 mM glucose (in complete medium) for 24 hours after which the cells were put into the hypoxia chamber, with 1% O_2, 5% CO_2 and 94% N_2, for 6 hours. Following this the ASCs were reoxygenated for 24 hours, at standard incubator conditions

(37°C and 5% CO_2), during which the EXs (unlabelled, EPC-derived or miR-126 overexpressed) were added.

Co-incubation of EXs with ASCs

The isolated EXs were resuspended in the ASC medium and added to the cells as per the experimental design. The labelled, unlabelled, EPC-EXs or miR-126 overexpressing EPC-EXs (miR-126 EPC-EXs) in concentrations 1 x 10^9, 2 x 10^9 or 3 x 10^9 EX particles/ml were resuspended in complete ASC medium and then co-incubated with the ASCs for 24 hours. Following this, the fluorescent images were recorded, or assays were performed.

EX uptake mechanism determination

As the literature suggests, there are various pathways for EX uptake which predominantly is based on the cell line being studied. To determine the EPC-EX uptake by ASCs, we focussed on the endocytic uptake narrowing it down to macropinocytosis, clathrin-mediated and caveolin-dependent pathways. For this, the cells were treated for 30 minutes with various inhibitors at specific concentrations. The inhibitors used were 80 μM dynasore (dynamin inhibitor), 5 μM LY290042 (macropinocytosis inhibitor), 10 μM pitstop 2 (clathrin inhibitor) and 200 μM genistein (caveolin inhibitor). After treatment with the inhibitors, the cells were washed twice and then the labelled EPC-EXs were co-incubated with these ASCs for 24 hours. Fluorescent images were obtained by fluorescence microscope and flow cytometry analysis was carried out through Accuri C6 flow cytometer.

miR-126 transfection

To generate miR-126 overexpressing EPC-EXs, the EPCs were transfected with miR-126 mimics (1 nm) using Dharmafect 1 transfection reagent for 48 hours in HEPC complete

growth medium with serum and antibiotics followed by replacing the complete medium with serum-free medium for 48 hours for release of EXs, isolated by ultracentrifugation at 170,000 x g for 90 minutes.

miR-126 expression analysis

miR-126 from the EPCs and EXs was extracted using the TRIzol reagent. After discarding the culture medium from the flask, 1ml TRIzol reagent was added to the flask and made to sit for a minute. This allowed the detachment of the cells, which were later transferred into a 1.5 ml microfuge tube. To this, 100 µl chloroform was added and shaken for 15 seconds until the solution turned pink. The tubes were allowed to stand for 10 minutes at room temperature and then centrifuged at 12,500 x g for 15 minutes at 4°C. Centrifugation resulted in separation of 3 layers, the topmost clear layer with the RNA extract, the middle cloudy layer with the DNA interphase and the bottom most later with the cell debris. The top clear layer was collected and transferred to a new tube to which 500 µl of pre-cooled isopropanol was added, mixed thoroughly via pipetting and allowed to rest at -20°C for 10 minutes. Following this, the tubes were centrifuged for 12,500 x g for 15 minutes at 4°C, and the supernatant was discarded. To the pellet, 1 ml of pre-cooled 75% ethanol was added and vortexed. The tube was then centrifuged at 7500 x g for 5 minutes at 4°C and the supernatant was discarded efficiently, after which the tube was dried in the ventilation hood for 5-10 minutes. The obtained RNA was the eluted with 30 µl of RNase free water by vigorous pipetting. The RNA concentration was measured using Nano drop 2000. cDNA was synthesized using PrimeScript RT reagent kit (Takara Bio Inc.) following the manufacturer's instructions. qRT-PCR was carried out using miR-126 specific primers and SYBR Premix Ex Taq kit (Takara Bio Inc.) on a real-time PCR instrument (Bio-Rad),

while RNA U6 was used as an internal control for this determination. Expression of miR-126 was calculated using $2^{-\Delta\Delta CT}$ method.

However, for the determination of miR-126 expression in the EXs, the similar steps were carried out as the EPCs except for the initial few and the concentrations of reagents used. After the isolation of EXs from the EPCs, the supernatant was discarded and to the tube 100 µl of TRIzol reagent was added. Following the same steps as before, 10 µl of chloroform, 50 µl of isopropanol and 100 µl of 75% ethanol were used in their respective steps. The RNA was eluted with 10 µl of RNase free water and the similar steps were followed as the EPCs.

Cell apoptosis assay

Cellular apoptosis was determined using Annexin V/ PI. Annexin V is a potent biomarker for cell apoptosis. It binds irreversibly to phosphatidyl serine, usually present on the inside of the plasma membrane in normal conditions, which is exposed during apoptosis because of scrambling of the plasma membrane. To determine apoptosis, ASCs were cultured in 6-well plate, injured with the HG + H/R model and then treated with EPC-EXs. ASCs without injury and EPC-EX treatment were treated as control. After this, the cells were detached from the wells, transferred to microfuge tubes and centrifuged at 300 x g for 6 minutes to obtain pellets. The pellets were resuspended in 100 µl of Annexin V binding buffer and vortexed. To the isotype control, 5 µl of isotype PE and 5 µl of isotype APC were added while to all the other groups 10 µl of conjugated PI and 5 µl of Annexin V were added. The tubes were vortex again and allowed to sit for 15 minutes in dark, at room temperature. The tubes were then centrifuged at 300 x g for 6 minutes, after which the supernatant was

discarded, and the antibody-labelled cells were resuspended in 100 µl of Annexin V binding buffer. The percent apoptosis was analysed using the flow cytometer.

Oxidative stress or intracellular ROS generation assay

Intracellular ROS generation, an effective method for determining oxidative stress in the cells was determined using dihydroethidium (DHE) staining in this study. DHE is a superoxide indicator which when oxidized primarily by a superoxide resulting in 2-hydroxyethidium. This compound intercalates with the DNA and stains the nucleus bright red, along with the cytosol. The ASCs were cultured in 6-well plate. After their reoxygenation phase of the injury model, they were incubated with 10 µM DHE solution (in dark) for 30 minutes at 37°C. The solution was then discarded, and the cells were washed with PBS twice, and fresh new complete medium was added to the wells. ASCs without injury and EX treatment were treated as control. The cells were then observed under fluorescence microscope and the percentage of DHE-positive cells was analysed using the flow cytometer.

Cell cytotoxicity assay

Cellular cytotoxicity determination is carried out using LDH cytotoxicity kit. This is a steadfast colorimetric assay that measures cytosolic LDH (lactate dehydrogenase), an oxidoreductase enzyme allowing the conversion of lactate to pyruvate, released into the medium by injured (or damaged) cells. A series of enzymatic reactions involving the released LDH result in generating a red fluorescent product, formazan. This resulting formazan can be measured at 490 nm. To determine the cell cytotoxicity, ASCs were cultured in 96-well plate (in triplicate wells), injured with the HG + H/R model and then treated with EPC-EXs. ASCs without injury and EPC-EX treatment were treated as control.

As per the manufacturer's instructions, the triplicate wells for each group were categorised into spontaneous LDH activity controls, maximum LDH activity controls and test LDH activity. To the spontaneous LDH activity control wells, 10 µl of ultrapure water was added and incubated at 37°C, 5% CO_2 for 30 minutes. Following this, 10 µl of lysis buffer was added to the maximum LDH activity control wells, mixed by gentle tapping and incubated at 37°C, 5% CO_2 for 45 minutes. After this, 50 µl of each sample medium was transferred to a new 96-well plate, to which 50 µl of reaction mixture was added and incubated for 30 minutes at room temperature, in dark. To stop the reaction, 50 µl of stop solution was added to each well and mixed by gentle tapping. Absorbance was measured at 490 nm and 680 nm and calculations for determination of percent cytotoxicity were carried out as per the manufacturer's instructions.

Lipid peroxidation assay

Lipid peroxidation refers to degradation of cellular lipids due to generation of reactive oxygen species within the cell. For the determination of lipid peroxidation, a sensitive fluorescent reporter BODIPY 581/591 C11 reagent (BODIPY dye) was used. The phenylbutadiene portion of the dye allows the shift of fluorescence emission peak from 590 nm-red to 510 nm-green upon oxidation. To determine the lipid peroxidation, ASCs were cultured in 6-well plate, injured with the HG + H/R model and then treated with EPC-EXs. ASCs without injury and EPC-EX treatment were treated as control. Following this, 10 µM BODIPY reagent was added to the wells and incubated for 30 minutes at 37°C. The media was removed followed by washing with PBS for 3 times. The ratio of reduction (590 nm)/oxidation (510 nm) was derived by reading the fluorescence intensities at the separate

wavelengths on Cytation 5 plate reader while the percent lipid peroxidation was analysed by the flow cytometer.

Statistical analysis

All data are expressed as mean ± SD of at least 3 experiments. Comparisons between two groups were performed using Student's *t*-test, while multiple comparisons were carried out by one-way ANOVA, followed by Tukey's post hoc test. A value of $P < 0.05$ was considered statistically significant. All the statistical analyses were performed using SigmaPlot (version 14.0) software.

V. RESULTS

PKH26 labelled EPC-EXs were uptaken by ASCs in concentration and time-dependent manner.

For the concentration-based study, cultured ASCs were co-incubated with PKH26 labelled EPC-EXs at 3 different concentrations- EPC-EX 1: 1 x 10^9 particles/ml, EPC-EX 2: 2 x 10^9 particles/ml and EPC-EX 3: 3 x 10^9 particles/ml for 24 hours. The fluorescence images were recorded after 24 hours indicating the labelled EPC-EX particles merged with the ASCs. The intensity of the exhibited red fluorescence suggesting that the uptaking ability of the EPC-EXs by the ASCs. The images suggested that the EPC-EXs were uptaken by the cells in a concentration-based pattern, wherein the fluorescence exhibited increased as the concentration of EPC-EXs increased (*Fig 16A*). However, for the time-dependent study, PKH26 labelled EPC-EXs were co-incubated with the ASCs at a concentration of 3 x 10^9 particles/ml for 24 hours, wherein fluorescent images were recorded for every 2 hours. Again, the fluorescence intensity proved to be the basis for the uptaking of these particles, merged with the cells. It was observed that the uptake was gradual as the time passed, greater uptake and fluorescence intensity was observed at 16-18 hours. This fluorescence gradually decreased until 24 hours suggesting the EXs being consumed by the cells, hence the loss in fluorescence (*Fig 16B*). Fluorescence fold change was recorded by flow cytometry at every time-point (*Fig 16C*).

A)

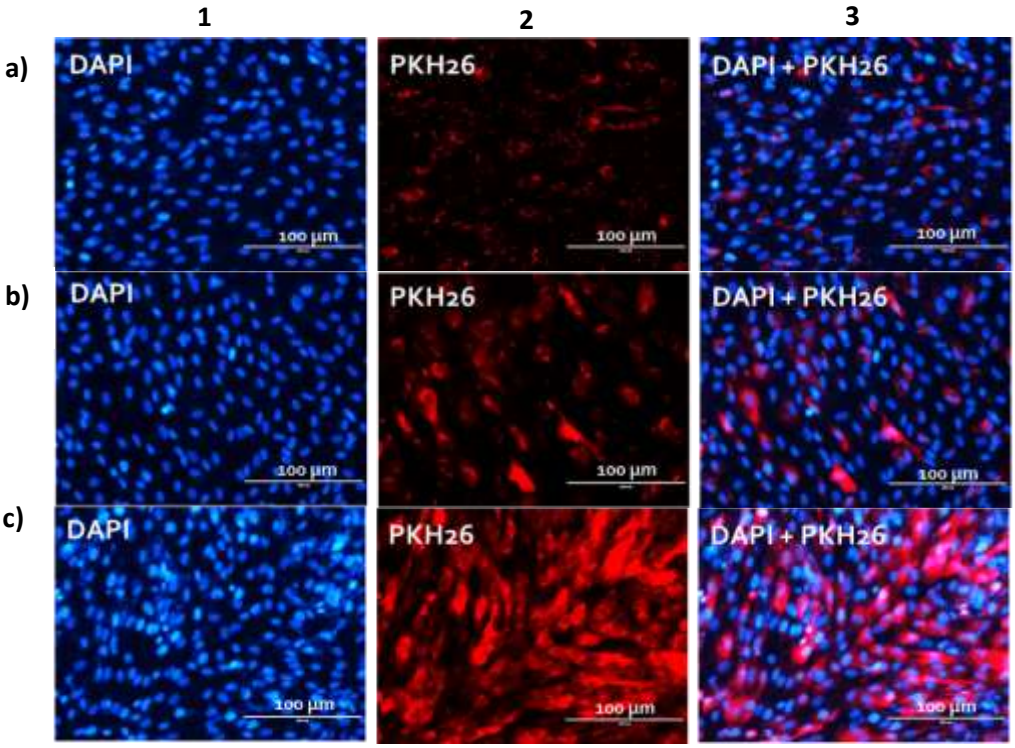
1
2
3
a)
b)
c)
DAPI
PKH26
DAPI + PKH26
100 µm

B)

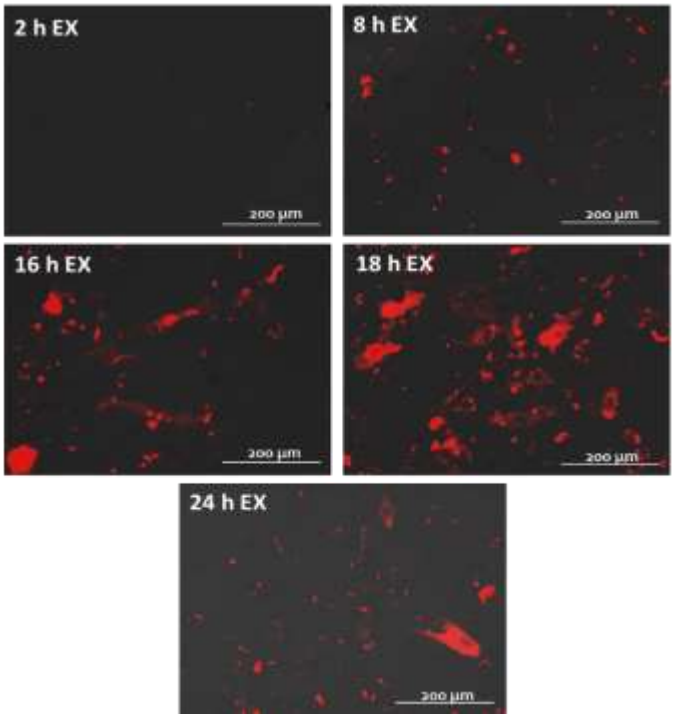
2 h EX
8 h EX
16 h EX
18 h EX
24 h EX
200 µm

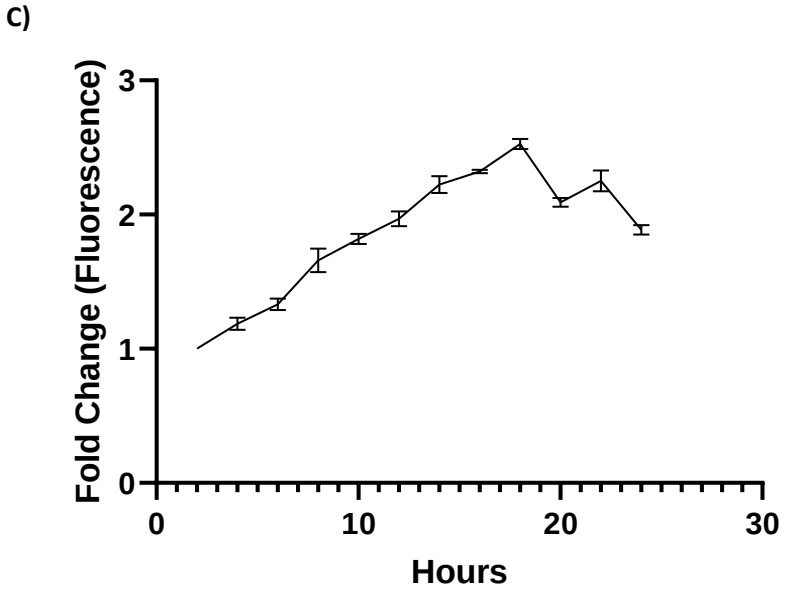

Fig 16: **Concentration and time dependent uptake of EPC-EXs by ASCs.** A) Representative images of PKH26 (red) stained EPC-EXs merged with ASCs, observed under the fluorescence microscope after 24 hours co-incubation. a-c1) DAPI (blue) stained nucleus of ASCs, a2) 1 x 10^9 PKH26 labelled EPC-EX particles/ml, b2) 2 x 10^9 PKH26 labelled EPC-EX particles/ml, c2) 3 x 10^9 PKH26 labelled EPC-EX particles/ml and a-c3) Overlay of images a with b. B) Representative images of PKH26 stained EPC-EXs merged with ASCs at various time points. C) Data summary representing fold change fluorescence for time-based uptake of PKH26 stained EPC-EXs by ASCs over 24 hours period. Fluorescence images were obtained every 2 hours along with flow cytometry data. Data represents mean ± SD, n = 3/ group.

EPC-EXs were uptaken by ASCs via macropinocytosis, caveolin-dependent and clathrin-mediated pathways.

To determine the uptake mechanisms, ASCs were treated with various synthetic drugs which allowed the inhibition of the uptake of PKH67 labelled EPC-EXs. These drugs were dynamin, macropinocytosis, clathrin and caveolin inhibitors. It was observed that the EPC-EX uptake significantly decreased after the treatment of these inhibitors in comparison to no treatment (Vehicle). ASCs were treated with vehicle (no treatment), 80 μM Dynasore (dynamin inhibitor), 10 μM Pitstop 2 (clathrin-mediated pathway inhibitor), 200 μM Genistein (caveolin-dependent pathway inhibitor) and 5 μM LY294002 (macropinocytosis inhibitor) for 30 minutes. Fluorescent images were recorded after 24 hours co-incubation (*Fig 17A*). The green fluorescence intensity suggested the uptake and merging of the EPC-EXs with the cells. Decreased fluorescence suggested decreased uptake of the labelled EPC-EXs by the cells hence, the inhibition of uptake had occurred after the drug activity. Fluorescence fold change was recorded for each group by flow cytometry (*Fig 17B*).

A)

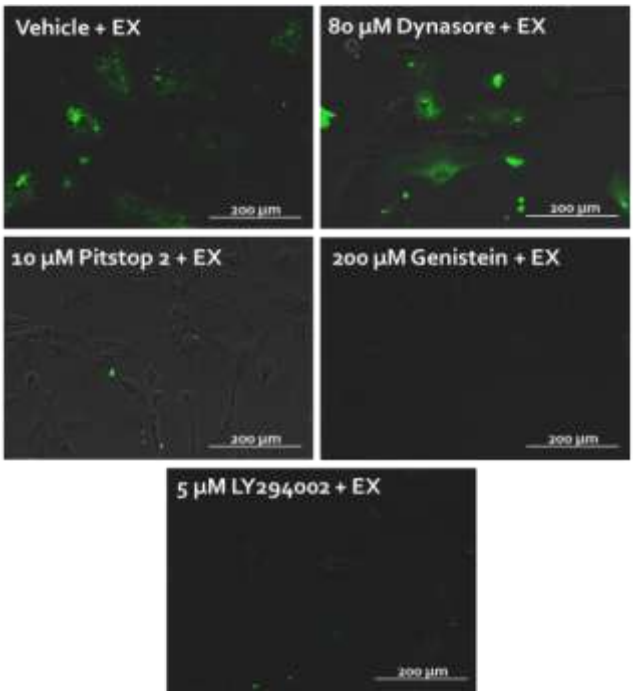

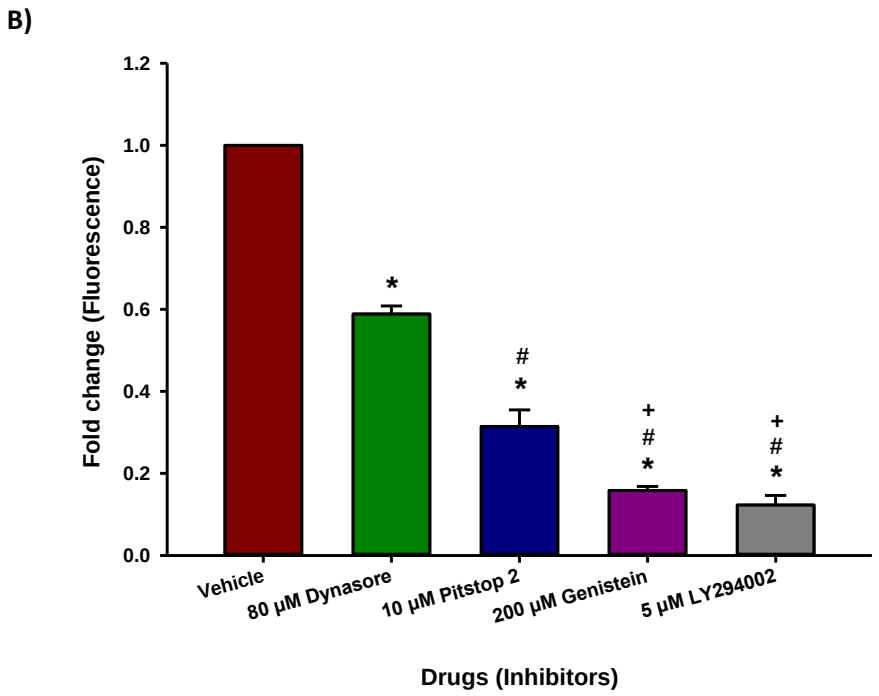

Fig 17: **Mechanisms of uptake for EPC-EXs by ASCs.** A) Representative fluorescent images of PKH67 labelled EPC-EXs merged with ASCs after 30 minutes treatment by vehicle, 80 µM Dynasore, 10 µM Pitstop 2, 200 µM Genistein and 5 µM LY294002, over an incubation period of 24 hours. B) Fluorescence intensity fold change levels recorded by flow cytometric analysis. Data represents mean ± SD, n = 4/group, *P (<0.05) v/s Vehicle, $^{\#}$P (<0.05) v/s 80 µM Dynasore, $^{+}$P (<0.05) v/s 10 µM Pitstop 2.

EPC-EXs decrease cellular apoptosis of HG + H/R injured ASCs.

To determine whether EPC-EXs could protect the ASCs from HG + H/R-induced injury, we assessed the apoptotic rate of ASCs co-incubated with 2 concentrations of EPC-EXs. The comparisons were based on the EPC-EX treatment provided to the ASCs after HG + H/R-induced injury. The test groups were control (no injury or EPC-EX treatment), HG (25 mM glucose), HG + H/R (injury without treatment), EPC-EX 1 (HG + H/R injured ASCs treated with 1 x 10^9 EPC-EX particles/ml) and EPC-EX 3 (HG + H/R injured ASCs treated with 3 x 10^9 EPC-EX particles/ml). Percent apoptosis determination was carried out through flow cytometry, focussing on the Annexin V +/ PI – (early apoptosis phase) in the quadrant 4 (Q4) (*Fig 18A*).It was found that the maximum concentration of EPC-EXs, the EPC-EX 3 group, significantly decreased cell apoptosis after HG + H/R-induced injury, thus protecting the cells against the injury (*Fig 18B*).

A)

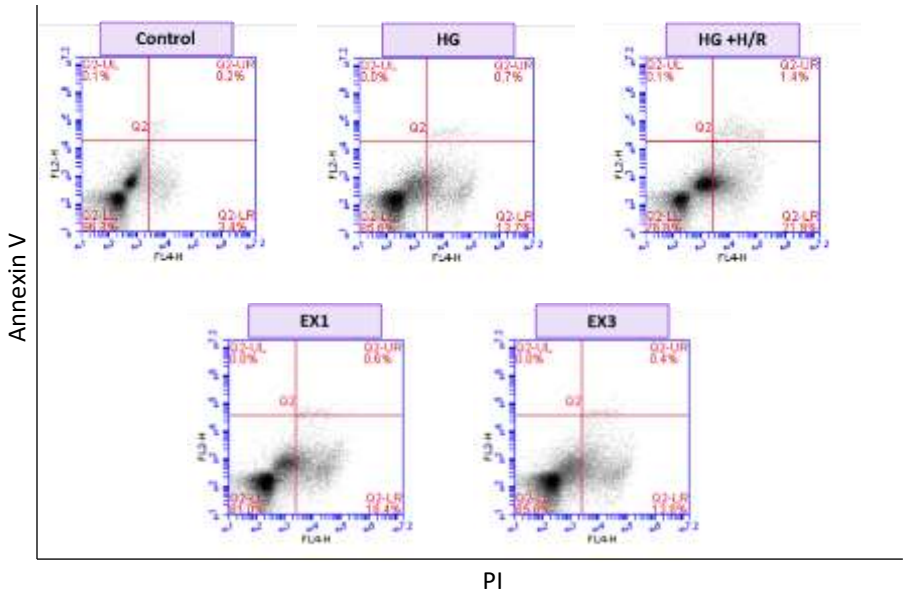

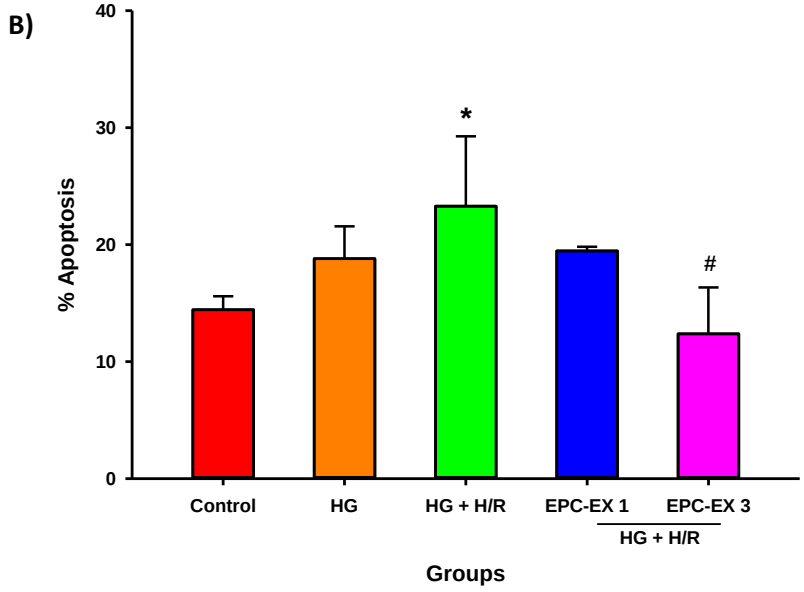

Fig 18: **Effect of EPC-EXs on HG + H/R-induced apoptosis of ASCs.** A) Representative flow cytometry plots for groups control, HG, HG + H/R, EPC-EX 1 and EPC-EX 3 with Annexin V on the y-axis and PI on the x-axis. B) Summarized data showing percent apoptosis of ASCs after HG + H/R-induced injury and EPC-EX treatment. EPC-EX 1: 1 x 10^9 EPC-EX particles/ml and EPC-EX 3: 3 x 10^9 EPC-EX particles/ml. Data are represented as mean ± SD, n = 12/group, *P (<0.05) v/s Control, $^{\#}$P (<0.05) v/s HG + H/R. Groups: Control (no injury or treatment), HG (High glucose), HG + H/R (High glucose + hypoxia/reoxygenation), EPC-EX (Endothelial progenitor cells-derived exosomes).

EPC-EXs decrease intracellular ROS generation due to HG + H/R-induced injury in ASCs.

ROS generation is the key factor for injury in the cells due to increased oxidative stress and intracellular lipid peroxidation. To deduce if EPC-EXs could protect the ASCs against HG + H/R-induced injury by attenuating the oxidative stress and lipid peroxidation, DHE and lipid peroxidation assays were carried out. ASCs were co-incubated with 2 different concentrations of EXs (EPC-EX 1 with 1 x 10^9 EPC-EX particles/ml and EPC-EX 3 with 3 x 10^9 EPC-EX particles/ml) after the injury, while these groups were compared with HG + H/R injured ASCs group. ASCs without injury and treatment were treated as controls. It was found that HG + H/R induced significant ROS generation and lipid peroxidation in the ASCs, while the maximum concentration of EPC-EXs, EPC-EX 3 group, significantly decreased the HG + H/R induced significant ROS generation and lipid peroxidation. Thus, suggesting an important therapeutic of EPC-EXs in reversing the damage due to oxidative stress and intracellular lipid peroxidation. DHE staining exhibited bright red fluorescence (*Fig 19A*), detected by fluorescence microscope while the percent DHE-positive cells were determined by flow cytometry (*Fig 19B*). To determine the intracellular lipid peroxidation, ratio of reduction (590 nm)/oxidation (510 nm) was derived by reading the fluorescence intensities (*Fig 19C*) while the percent lipid peroxidation was determined by flow cytometry analysis (*Fig 19D*).

A)

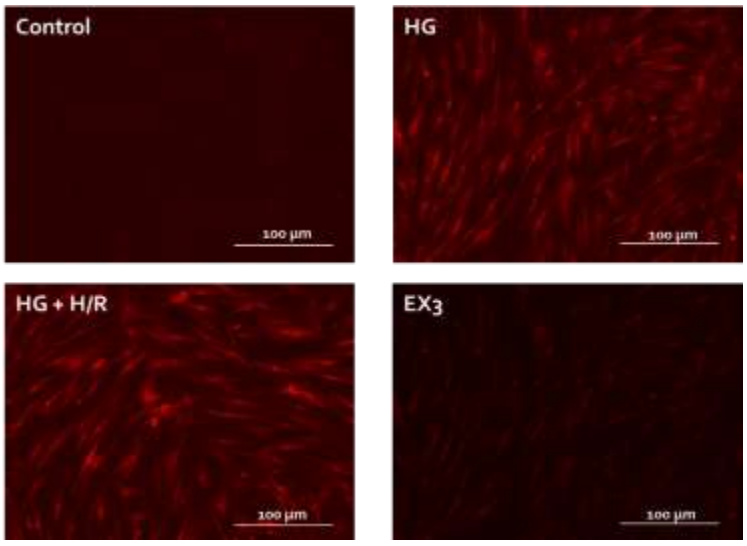
Control
100 µm
HG
100 µm
HG + H/R
100 µm
EX3
100 µm

B)

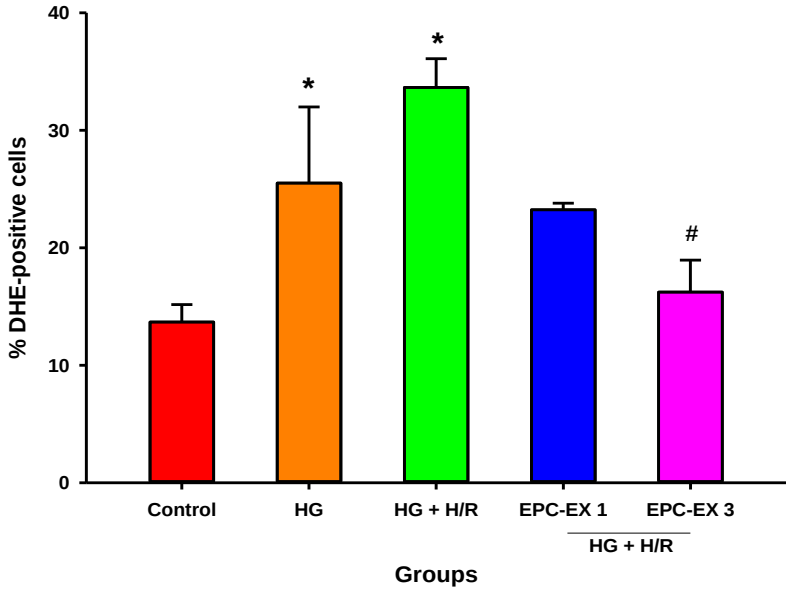
40
30
20
10
0
% DHE-positive cells
*
*
#
Control
HG
HG + H/R
EPC-EX 1
EPC-EX 3
HG + H/R
Groups

C)

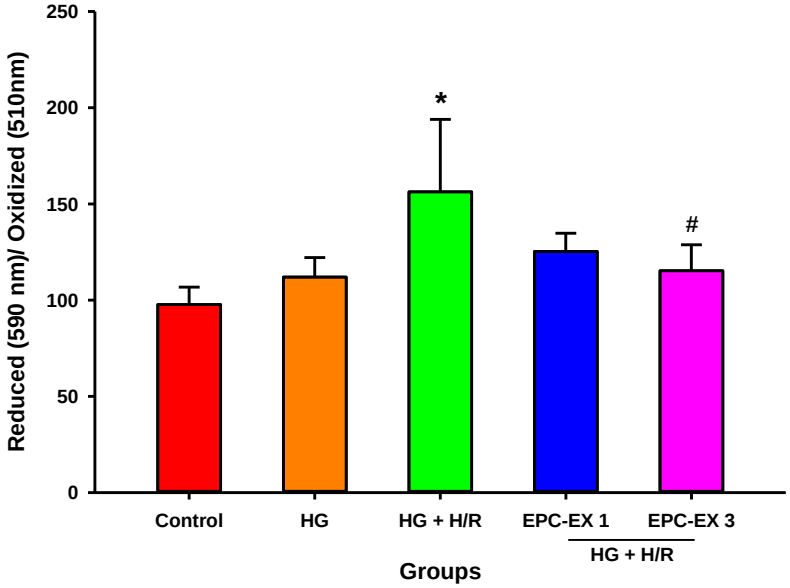
Reduced (590 nm)/ Oxidized (510nm)
250
200
150
100
50
0
*
#
Control
HG
HG + H/R
EPC-EX 1
EPC-EX 3
HG + H/R
Groups

D)

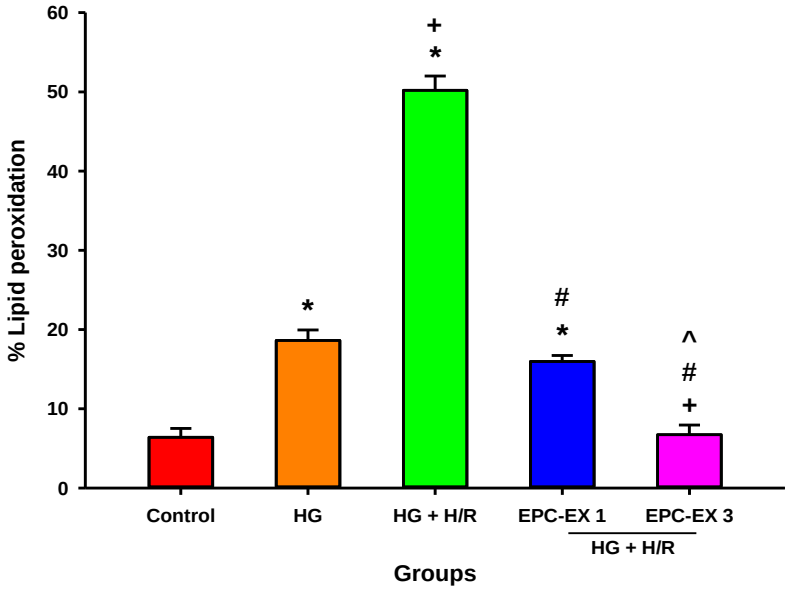
% Lipid peroxidation
60
50
40
30
20
10
0
+
*
*
#
*
^
#
+
Control
HG
HG + H/R
EPC-EX 1
EPC-EX 3
HG + H/R
Groups

Fig 19: **Effect of EPC-EXs on oxidative stress and lipid peroxidation.** A) Representative DHE staining fluorescent images exhibiting bright red fluorescence. B) Summarized flow cytometry analysis representing percent DHE-positive cells. C) Fluorescence intensity data summary representing ratio of reduction (590 nm)/oxidation (510 nm). D) Summarized flow cytometry analysis representing percent intracellular lipid peroxidation. EPC-EX 1: 1 x 10^9 EPC-EX particles/ml, EPC-EX 3: 3 x 10^9 EPC-EX particles/ml. Data are represented as mean ± SD, n = 6-10/group, *P (<0.05) v/s Control, $^{\#}$P (<0.05) v/s HG + H/R, $^{+}$P (<0.05) v/s HG, ^P (<0.05) v/s EPC-EX 1. Groups: Control (no injury or treatment), HG (High glucose), HG + H/R (High glucose + hypoxia/reoxygenation), EPC-EX (Endothelial progenitor cells-derived exosomes).

EPC-EXs decrease cell cytotoxicity of HG + H/R injured ASCs.

To determine the protective effect of EPC-EXs on cell cytotoxicity levels, we assessed the cell cytotoxicity for ASCs which were co-incubated with 2 different concentrations of EPC-EXs (EPC-EX 1 with 1 x 10^9 EPC-EX particles/ml and EPC-EX 3 with 3 x 10^9 EPC-EX particles/ml) after the injury, while these groups were compared with HG + H/R injured ASCs group. ASCs without injury and treatment were treated as controls. The colorimetric assay performed on these groups suggested that there is increased cytotoxicity due to the HG + H/R injury, however EPC-EX 3 significantly decreases the percent cytotoxicity

levels for the ASCs, thus protecting the cells from further damage. Percent cytotoxicity was determined by the colorimetric LDH assay, reading the absorbance at 490 nm and 680 nm and performing the calculations as per the manufacturer's instructions (*Fig 20*).

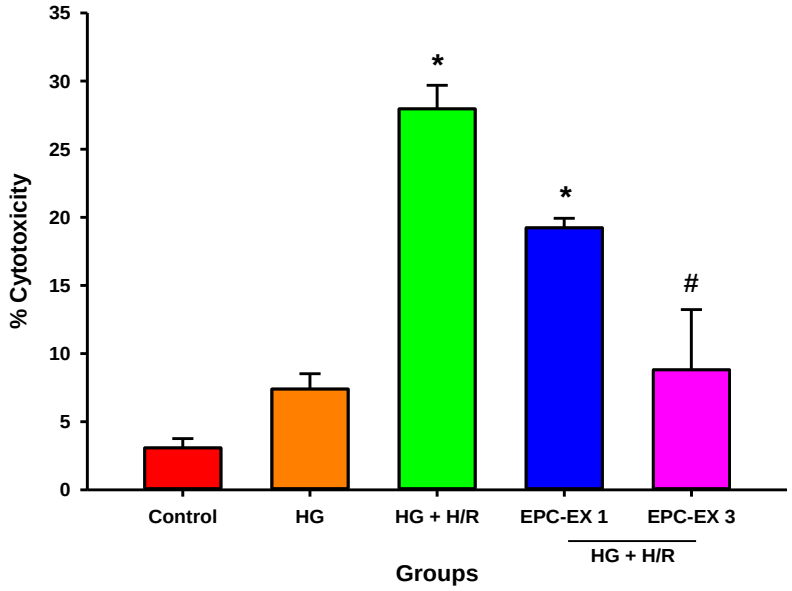

Fig 20: **Effect of EPC-EXs on cell cytotoxicity after HG + H/R injury of ASCs.** Summarized colorimetric absorbance readout data calculated to represent percent cytotoxicity. EPC-EX 1: 1 x 10^9 EPC-EX particles/ml, EPC-EX 3: 3 x 10^9 EPC-EX particles/ml. Data are represented as mean ± SD, n = 6/group, *P (<0.05) v/s Control, $^{\#}$P (<0.05) v/s HG + H/R. Groups: Control (no injury or treatment), HG (High glucose), HG + H/R (High glucose + hypoxia/reoxygenation), EPC-EX (Endothelial progenitor cells-derived exosomes).

Transfection of miR-126 mimics leads to overexpression of miR-126 in EPCs and EPC-EXs.

In order to obtain miR-126 overexpressing EPC-EXs, EPCs were transfected and EPC-EXs were isolated. The level of miR-126 in both cells and EXs were analysed by qRT-PCR. The level of miR-126 in transfected EPCs was found to be almost 30 folds while that for the isolated EPC-EXs was found to be around 5 folds (*Fig 21*).

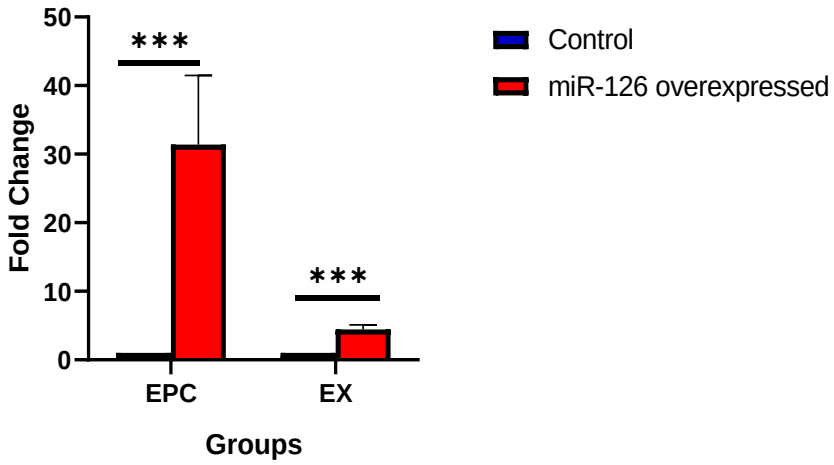

Fig 21: **Effect of miR-126 mimic transfection on its expression**. Summarized data represents the fold change in levels of miR-126 expression in miR-126 transfected EPCs and isolated EPC-EXs in comparison to the untransfected control. Data are represented as mean ± SD, n = 4/group, ***P (<0.05).

miR-126 EPC-EXs decrease cellular apoptosis of HG + H/R injured ASCs.

To determine the effect of miR-126 EPC-EXs on the apoptosis of HG + H/R injured ASCs, Annexin V/ PI apoptosis assay was conducted. The comparisons were based on the EX treatments provided to the ASCs after HG + H/R-induced injury. The test groups were control (no injury or EPC-EX treatment), HG (25 mM glucose), HG + H/R (injury without treatment), EPC-EX (HG + H/R injured ASCs treated with 3 x 10^9 EPC-EX particles/ml)

and miR-126 EPC-EX (HG + H/R injured ASCs treated with 3 x 10^9 miR-126 overexpressing EPC-EX particles/ml). Percent apoptosis determination was carried out through flow cytometry, focussing on the Annexin V +/ PI – (early apoptosis phase) in the quadrant 4 (Q4) (*Fig 22A*). It was found that miR-126 EPC-EXs significantly decrease the ASC apoptotic rate, however the results were not significant in comparison to the EPC-EX group (*Fig 22B*).

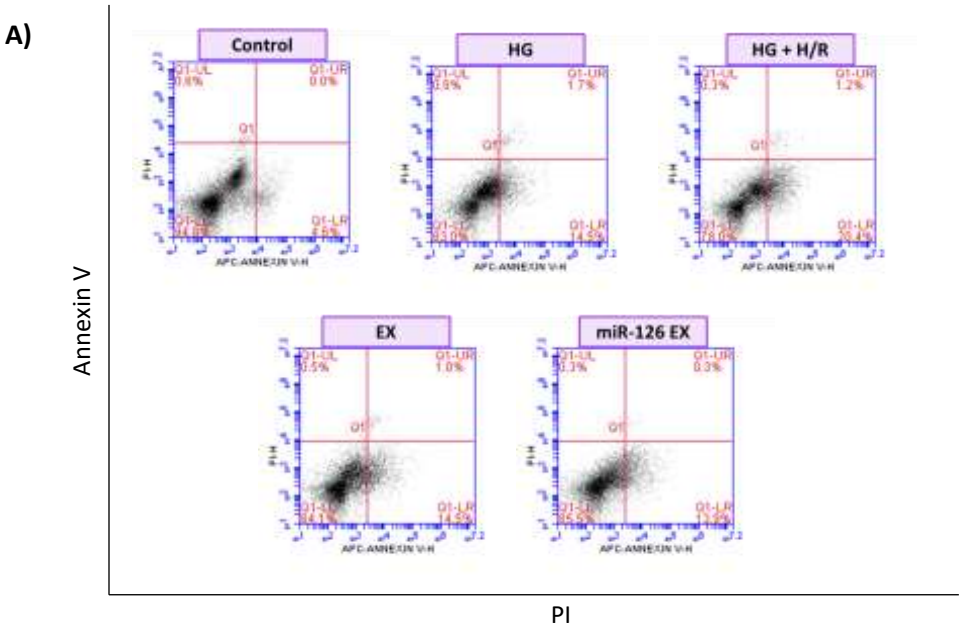

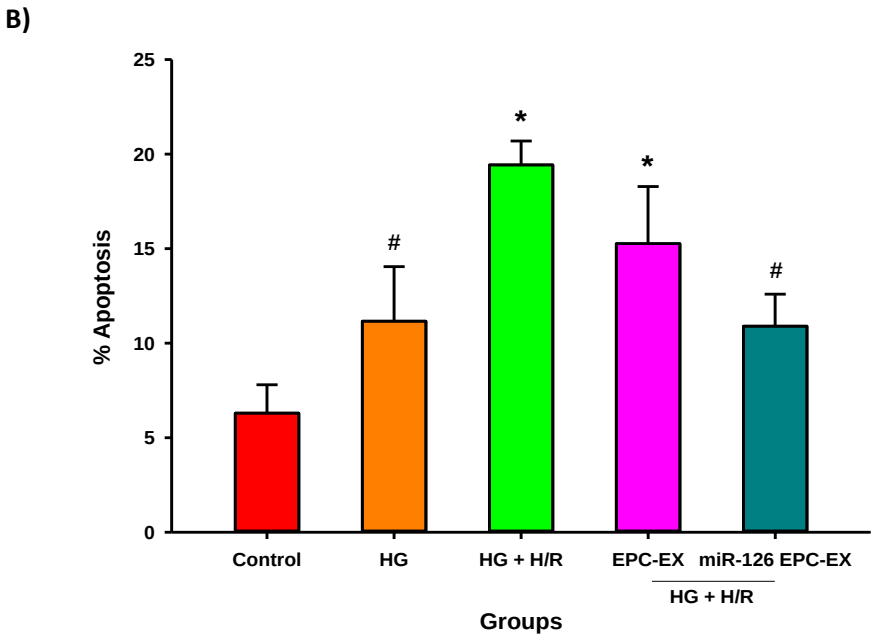

Fig 22: **Effect of miR-126 EPC-EXs on HG + H/R-induced apoptosis of ASCs.** A) Representative flow cytometry plots for groups control, HG, HG + H/R, EPC-EX and miR-126 EPC-EX with Annexin V on the y-axis and PI on the x-axis. B) Summarized data showing percent apoptosis of ASCs after HG + H/R-induced injury and EPC-EX treatment. EPC-EX: 3 x 10^9 EPC-EX particles/ml and miR-126 EPC-EX: 3 x 10^9 miR-126 overexpressing EPC-EX particles/ml. Data are represented as mean ± SD, n = 6/group, *P (<0.05) v/s Control, $^{\#}$P (<0.05) v/s HG + H/R. Groups: Control (no injury or treatment), HG (High glucose), HG + H/R (High glucose + hypoxia/reoxygenation), EPC-EX (Endothelial progenitor cells-derived exosomes), miR-126 EPC-EX (microRNA 126 overexpressing EPC-EX).

miR-126 EPC-EXs decrease HG + H/R induced intracellular ROS generation in ASCs.

As discussed previously, ROS generation is a key factor in cell damage and death. To determine if miR-126 EPC-EXs have an effect on the ROS generation, thus affecting the oxidative stress and lipid peroxidation, DHE and lipid peroxidation assays were performed. It was found that miR-126 EPC-EXs decrease the ROS generation significantly, however there was no significant difference observed between the effects of groups EPC-EXs and miR-126 EPC-EXs. DHE staining exhibited bright red fluorescence (*Fig 23A*), detected by fluorescence microscope while the percent DHE-positive cells were determined by flow cytometry (*Fig 23B*). To determine the intracellular lipid peroxidation, ratio of reduction (590 nm)/oxidation (510 nm) was derived by reading the fluorescence intensities (*Fig 23C*) while the percent lipid peroxidation was determined by flow cytometry analysis (*Fig 23D*).

A)

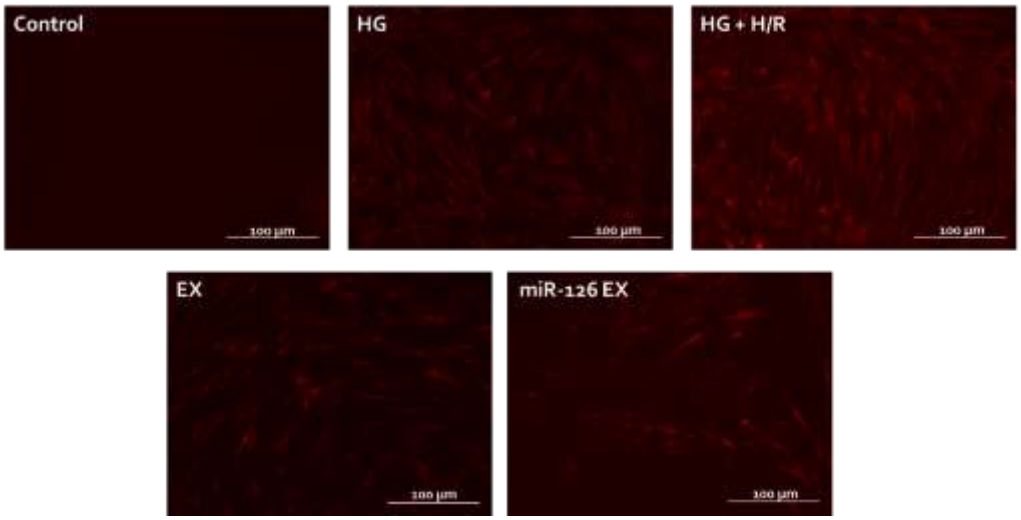

B)

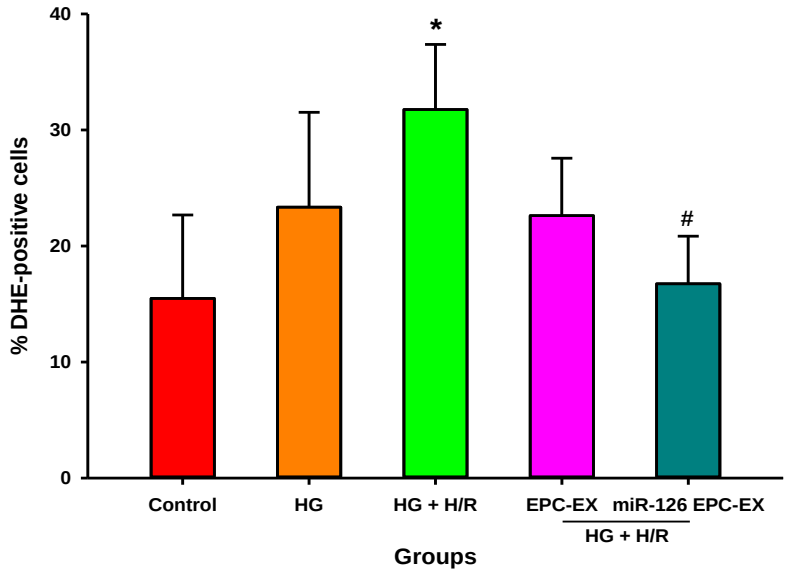
40
30
20
10
0
% DHE-positive cells
*
#
Control
HG
HG + H/R
EPC-EX
miR-126 EPC-EX
HG + H/R
Groups

C)

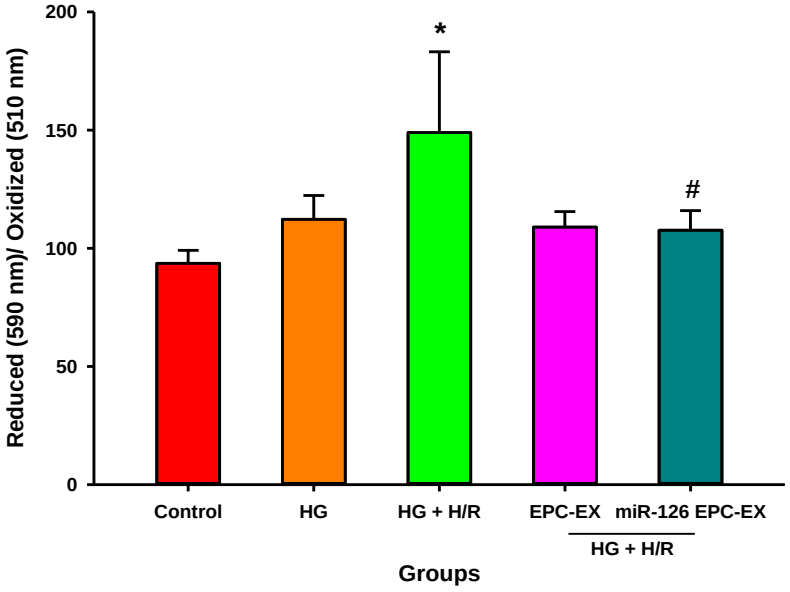
200
150
100
50
0
Reduced (590 nm)/ Oxidized (510 nm)
*
#
Control
HG
HG + H/R
EPC-EX
miR-126 EPC-EX
HG + H/R
Groups

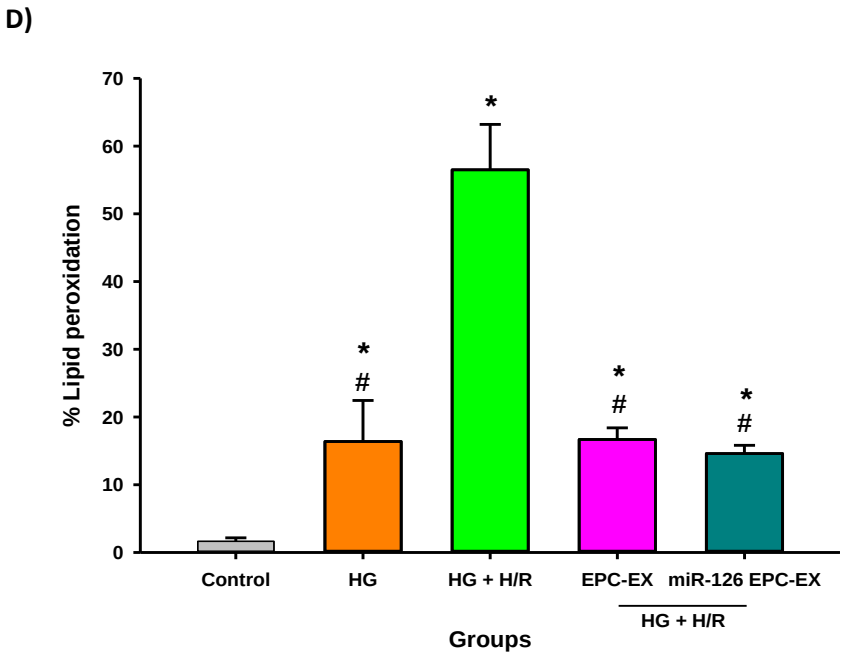

Fig 23: **Effect of miR-126 EPC-EXs on oxidative stress and lipid peroxidation.**

A) Representative DHE staining fluorescent images exhibiting bright red fluorescence. B) Summarized flow cytometry analysis representing percent DHE-positive cells. C) Fluorescence intensity data summary representing ratio of reduction (590 nm)/oxidation (510 nm). D) Summarized flow cytometry analysis representing percent intracellular lipid peroxidation. EPC-EX: 3 x 10^9 EPC-EX particles/ml, miR-126 EPC-EX: 3 x 10^9 miR-126 overexpressing EPC-EX particles/ml. Data are represented as mean ± SD, n = 6-10/group, *P (<0.05) v/s Control, $^{\#}$P (<0.05) v/s HG + H/R. Groups: Control (no injury or treatment), HG (High glucose), HG + H/R (High glucose + hypoxia/reoxygenation), EPC-EX (Endothelial progenitor cells-derived exosomes), miR-126 EPC-EX (microRNA 126 overexpressing EPC-EX).

miR-126 EPC-EXs decrease cell cytotoxicity of HG + H/R injured ASCs in comparison to EPC-EXs.

To deduce the effect of the overexpressed miR-126 in the miR-126 EPC-EXs on cellular cytotoxicity, we assessed the cell cytotoxicity for ASCs co-incubated with miR-126 EPC-EXs (3×10^9 particles/ml) after the injury, while these groups were compared with HG + H/R injured ASCs group as well as the EPC-EX treated injured group. ASCs without injury and treatment were treated as controls. The colorimetric assay performed on these groups suggested that there is increased cytotoxicity due to the HG + H/R injury, however miR-126 EPC-EX significantly decreases the percent cytotoxicity levels for the ASCs, thus protecting the cells from further damage. The interesting observation here was the data showing significant difference in reduction of cytotoxicity in miR-126 EPC-EX and EPC-EX groups, suggesting the enhanced effect of miR-126 EPC-EXs on the damaged cells. Percent cytotoxicity was determined by the colorimetric LDH assay, reading the absorbance at 490 nm and 680 nm and performing the calculations as per the manufacturer's instructions (*Fig 24*).

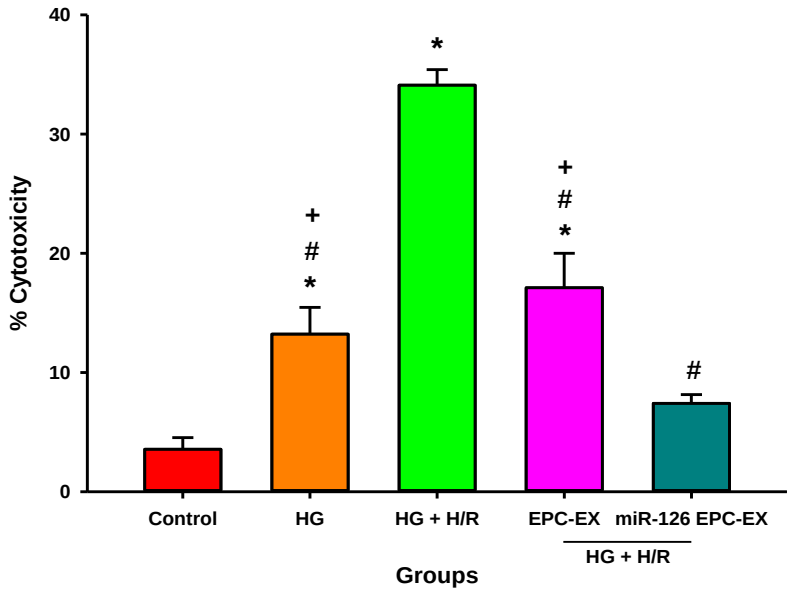

Fig 24: **Effect of miR-126 EPC-EXs on cell cytotoxicity after HG + H/R injury of ASCs.** Summarized colorimetric absorbance readout data calculated to represent percent cytotoxicity. EPC-EX: 3 x 10^9 EPC-EX particles/ml, miR-126 EPC-EX: 3 x 10^9 miR-126 overexpressing EPC-EX particles/ml. Data are represented as mean ± SD, n = 5/group, *P (<0.05) v/s Control, $^{\#}$P (<0.05) v/s HG + H/R, $^{+}$P (<0.05) v/s miR-126 EPC-EX. Groups: Control (no injury or treatment), HG (High glucose), HG + H/R (High glucose + hypoxia/reoxygenation), EPC-EX (Endothelial progenitor cells-derived exosome), miR-126 EPC-EX (microRNA-126 overexpressing EPC-EX).

VI. DISCUSSION

EXs are nanosized, extracellular vesicles released by almost all cells in physiological as well as stressful conditions. These phospholipid bilayer vesicles, generated within the endosomes of the cells and released into the extracellular space via fusion with the plasma membrane, are involved in cell-to-cell signalling and found to contain DNA, RNA, mRNA, miRNA, lipds and proteins, which are responsible for the transfer of information. This property of EXs exemplifies them as novel therapeutic agents also, qualifying them for being involved in drug delivery. In this study we isolated the EXs from EPCs which were uptaken by the ASCs via macropinocytosis, clathrin-mediated endocytosis and caveolin-dependent endocytosis mechanisms (*Fig 17*). Also, the uptake was increased with increased time of co-incubation and concentration of EPC-EXs, thus highest uptake was observed at the concentration of 3×10^9 particles/ml (*Fig 16A*) at 16-18 hours (*Fig 16B, 16C*), after which the levels decreased suggesting the consumption of these EPC-EXs by the cells. These results suggest that EPC-EXs are effectively taken up by the cells in a concentration and time-dependent pattern by 3 different uptake mechanisms (*Fig 16, 17*)

The in-vitro representation of ischemic stroke due to diabetes was achieved through HG + H/R induced injury of ASCs. 25 mM glucose enriched medium correlates with the physiological condition of diabetes while hypoxia, 1% O_2, 5% CO_2, 94% N_2, for 6 hours followed by 24 hours or reoxygenation at standard incubator conditions depicts the physiological condition of ischemic stroke. H/R-induced injury lead to an increase in the

ROS, apoptosis, while it decreased NO and eNOS production in the hb-ECs. However, the EPC derived microvesicles (MVs) when co-incubated with the H/R damaged ECs, it resulted in increased eNOS, NO production while rescuing the cells from ROS overproduction and apoptosis [68]. Similar results were obtained in our study, however we wanted to test the effect of EPC-EXs on HG + H/R injured ASCs. HG + H/R injury induction resulted in early apoptosis of a population of cells which decreased when treatment with 1 x 10^9 EPC-EX particles/ml was carried out. The population further decreased with a treatment of higher concentration, that is 3 x 10^9 EPC-EX particles/ml (Fig 18A). Further summarized data suggested that EPC-EXs at a concentration of 3 x 10^9 EPC-EX particles/ml, significantly decrease the apoptosis rate of ASCs (Fig 18B). These results suggest that EPC-EXs protect the HG + H/R injured ASCs from apoptosis and help them recover (*Fig 18*). ROS is one of the major players' responsible for cell damage and death after HG + H/R. In our study, we found that 3 x 10^9 EPC-EX particles/ml significantly decreased the ROS generation represented by the bright red fluorescence and the DHE-positive cells, however the lower concentration of EPC-EXs could not reduce the ROS generation that significantly (*Fig 19A, 19B*). EPC-EXs were also found to decrease the ratio of reduction/oxidation of intracellular lipids and lipid peroxidation within the ASCs injured by HG + H/R. The colorimetric results suggested that EPC-EXs with the concentration 3 x 10^9 EPC-EX particles/ml decreased the ratio which was elevated due to HG + H/R injury (*Fig 19C*). While, the flow cytometry results proposed the increase in lipid peroxidation after the injury which was significantly decreased by the EPC-EXs. EPC-EX concentration of 1 x 10^9 EPC-EX particles/ml decreased the lipid peroxidation by almost 30% while, 3 x 10^9 EPC-EX particles/ml reduced the lipid peroxidation by almost

40% which was significantly different to the lower concentration of EPC-EXs used (*Fig 19D*). These results demonstrate the therapeutic efficacy of EPC-EXs in attenuating the ROS generation by HG + H/R-induced injury (*Fig 19*). Cell cytotoxicity was another parameter which was tested in our study involving the ASCs and the EPC-EXs. We found a decrease in cell cytotoxicity after the treatment of injured ASCs with that EPC-EXs, however only the EPC-EX concentration of 3 x 10^9 EPC-EX particles/ml significantly reduced the cytotoxicity (*Fig 20*).

As mentioned previously, EXs are composed of biomolecules such as DNA, RNA, lipid proteins, miRNA are short non-coding RNAs. miR-126 is a highly expressed endothelial specific miRNA, located on the human chromosome 9. It has been noted that miR-126 has proved to therapeutically efficacious in cerebral impairment due to ischemia [64]. miR-126 is endogenously expressed in EXs. In our study, as we are focussing on EPC-EXs as therapeutic agents, we overexpressed the levels of miR-126 in both the cells as well as the EXs derived from these cells. The results from this study showed ~30-fold increase in miR-126 levels in the transfected cells when compared to the controls, while a ~5-fold increase was observed in the EPC-EXs derived from the transfected cells to that of the control (*Fig 21*). This indicates that the miR-126 is effectively transfected and overexpressed in the EPC-EXs which could in turn provide therapeutic efficacy.

miR-126 regulates several functions mainly being involved in angiogenesis, cell survival and maintenance of vascular structure. Hence, it has proven to be beneficial in treating various vascular diseases. It plays a vital part in recovery after ischemia-reperfusion injury. miR-126 directly targets vascular endothelial growth factor A (VEGF-A), vascular cell adhesion molecule 1 (VCAM-1), insulin receptor substrate 1 (IRS-1), sprouty related

EVH1 domain containing 1 (SPRED-1) and PI3K (phosphoinositol-2-kinase) regulatory subunit p85 beta (PIK3R2). In our study, we determined the effect of miR-126 overexpressing EPC-EXs on HG + H/R injured astrocytes. The data demonstrated a decrease in ASC apoptosis after treatment with miR-126 EPC-EXs at a concentration of 3 x 10^9 miR-126 overexpressing EPC-EX particles/ml. However, the decrease due to miR-126 was not significantly different from the effect of EPC-EXs on injured ASCs (Fig 22A, 22B). This suggested that miR-126 EPC-EXs also exhibit a protective effect towards HG + H/R injured ASCs. Similarly, miR-126 EPC-EXs, at a concentration of 3 x 10^9 miR-126 overexpressing EPC-EX particles/ml, significantly reduced the ROS generation elucidated by the bright red DHE-stained cells (*Fig 23A*) as well as the summarized flow cytometry data (*Fig 23B*). Again, the effect of miR-126 EPC-EXs was significant in comparison to the injured group but not to the EPC-EXs group. This data proclaims that the miR-126 EPC-EXs are responsible for protecting the ASCs against oxidative stress. While, the lipid peroxidation and cell cytotoxicity results showed a significant difference in the effect of EPC-EXs on HG + H/R injured ASCs, by reduction in the reduced/oxidized ratio (*Fig 23C*), lipid peroxidation (*Fig 23D*) and cell cytotoxicity (*Fig 24*). However, the interesting part was miR-126 EPC-EXs, at a concentration of 3 x 10^9 miR-126 overexpressing EPC-EX particles/ml, significantly decreased the lipid peroxidation and cell cytotoxicity in comparison to EPC-EXs at the same concentration. This intriguing data suggested that the enhanced protective effects of miR-126 EPC-EXs, in comparison to EPC-EXs, may be due to the overexpressing miR-126.

Through the entire study, it was proved that EPC-EXs do project a protective effect on HG + H/R injured ASCs. However, the enhanced effects due to miR-126 EPC-EXs remain

unclear as an inhibitor of miR-126 was not employed here in order to determine the enhanced effect exerted was solely due to miR-126 or there were other factors responsible for the same. This would be an interesting part to investigate ahead in this study, along with the determination of the potential targets for miR-126 in the ASCs.

VII. CONCLUSIONS

Our data for this study demonstrates that the EPC-EXs are efficiently uptaken by the ASCs in a time and concentration dependent manner. The major pathways for mechanism of EPC-EX uptake in ASCs are macropinocytosis, clathrin-mediated endocytosis and caveolin-dependent endocytosis. HG + H/R-induced injury to the ASCs lead to an increase in apoptosis, oxidative stress, lipid peroxidation and cell cytotoxicity. However, the treatment of EPC-EXs resulted in reduced apoptosis, oxidative stress, lipid peroxidation and cytotoxicity thus, suggesting that EPC-EXs protect the ASCs from HG + H/R-induced injury. The data also suggested that EPCs transfected with miR-126 mimics release miR-126 overexpressing EPC-EXs. Treatment of injured ASCs with miR-126 EPC-EXs also resulted in reduction of apoptosis, oxidative stress, lipid peroxidation and cytotoxicity suggesting the protective effect of miR-126 EPC-EXs on HG + H/R injured ASCs.

VIII. REFERENCES

1. Stroke Facts | cdc.gov. Cdc.gov. https://www.cdc.gov/stroke/facts.htm.

2. Benjamin E, Blaha M, Chiuve S et al. Heart Disease and Stroke Statistics—2017 Update: A Report From the American Heart Association.

3. Stroke: Hope Through Research | National Institute of Neurological Disorders and Stroke. Ninds.nih.gov. https://www.ninds.nih.gov/Disorders/Patient-Caregiver-Education/Hope-Through-Research/Stroke-Hope-Through-Research.

4. Onwuekwe I, Ezeala-Adikaibe B. Ischemic stroke and neuroprotection. Ann Med Health Sci Res. 2012;2(2):186. doi:10.4103/2141-9248.105669

5. Stroke: classification and diagnosis. Pharmaceutical Journal. https://www.pharmaceutical-journal.com/learning/learning-article/stroke-classification-and-diagnosis/11080450.article?firstPass=false.

6. Introduction | Stroke and transient ischaemic attack in over 16s: diagnosis and initial management | Guidance | NICE. Nice.org.uk. https://www.nice.org.uk/guidance/cg68/chapter/Introduction.

7. Ischemic Strokes (Clots). www.strokeassociation.org. https://www.strokeassociation.org/en/about-stroke/types-of-stroke/ischemic-stroke-clots.

8. Ischemic Stroke. Cedars-sinai.edu. https://www.cedars-sinai.edu/Patients/Health-Conditions/Ischemic-Stroke.aspx.

9. Stroke. Department of Rehabilitation and Regenerative Medicine. http://www.cumc.columbia.edu/rehab/staywell/document.php?id=34191.

10. Ovbiagele B, Nguyen-Huynh M. Stroke Epidemiology: Advancing Our Understanding of Disease Mechanism and Therapy. Neurotherapeutics. 2011;8(3):319-329. doi:10.1007/s13311-011-0053-1

11. Allen C, Bayraktutan U. Risk Factors for Ischaemic Stroke. International Journal of Stroke. 2008;3(2):105-116. doi:10.1111/j.1747-4949.2008.00187.x

12. Choudhury M, Chowdhury M, Nayeem A, Jahan W. Modifiable and Non-Modifiable Risk Factors of Stroke: A Review Update. Journal of National Institute of Neurosciences Bangladesh. 2015;1(1):22-26. doi:10.3329/jninb.v1i1.22944

13. Stroke - Diagnosis and treatment - Mayo Clinic. Mayoclinic.org. https://www.mayoclinic.org/diseases-conditions/stroke/diagnosis-treatment/drc-20350119.

14. Stroke - Diagnosis, Evaluation and Treatment. Radiologyinfo.org. https://www.radiologyinfo.org/en/info.cfm?pg=stroke.

15. Ji R, Schwamm LH, Pervez MA, Singhal AB. Ischemic Stroke and Transient Ischemic Attack in Young Adults: Risk Factors, Diagnostic Yield, Neuroimaging, and Thrombolysis. JAMA Neurol. 2013;70(1):51–57. doi:10.1001/jamaneurol.2013.575

16. Adams HP. Treating Ischemic Stroke as an Emergency. Arch Neurol. 1998;55(4):457–461. doi:10.1001/archneur.55.4.457

17. Roth J. Recombinant Tissue Plasminogen Activator for the Treatment of Acute Ischemic Stroke. Baylor University Medical Center Proceedings. 2011;24(3):257-259. doi:10.1080/08998280.2011.11928729

18. Jilani T, Siddiqui A. Tissue Plasminogen Activator. Ncbi.nlm.nih.gov. https://www.ncbi.nlm.nih.gov/books/NBK507917/. Published 2019.

19. Gravanis I, Tsirka S. Tissue-type plasminogen activator as a therapeutic target in stroke. Expert Opin Ther Targets. 2008;12(2):159-170. doi:10.1517/14728222.12.2.159

20. Mechanism of Action - Cathflo® Activase® (alteplase). Cathflo.com. https://www.cathflo.com/catheter-management/mechanism-of-action.html.

21. Wang J, Yang W, Xie H, Song Y, Li Y, Wang L. Ischemic stroke and repair: current trends in research and tissue engineering treatments. Regen Med Res. 2014;2(1):3. doi:10.1186/2050-490x-2-3

22. Chang P, Prabhakaran S. Recent advances in the management of acute ischemic stroke. F1000Res. 2017;6:484. doi:10.12688/f1000research.9191.1

23. Aynalem S, Zeleke A. Prevalence of Diabetes Mellitus and Its Risk Factors among Individuals Aged 15 Years and Above in Mizan-Aman Town, Southwest Ethiopia, 2016: A Cross Sectional Study. Int J Endocrinol. 2018;2018:1-7. doi:10.1155/2018/9317987

24. Association A. Statistics About Diabetes. American Diabetes Association. http://www.diabetes.org/diabetes-basics/statistics/.

25. Deshpande A, Harris-Hayes M, Schootman M. Epidemiology of Diabetes and Diabetes-Related Complications. Phys Ther. 2008;88(11):1254-1264. doi:10.2522/ptj.20080020

26. Diabetes. Who.int. https://www.who.int/news-room/fact-sheets/detail/diabetes.

27. Bennett P. The Diagnosis of Diabetes: New International Classification and Diagnostic Criteria. Annu Rev Med. 1983;34(1):295-309. doi:10.1146/annurev.me.34.020183.001455

28. Diagnosis and Classification of Diabetes Mellitus. Diabetes Care. 2013;37(Supplement_1):S81-S90. doi:10.2337/dc14-s081

29. Goldenberg R, Punthakee Z. Definition, Classification and Diagnosis of Diabetes, Prediabetes and Metabolic Syndrome. Can J Diabetes. 2013;37:S8-S11. doi:10.1016/j.jcjd.2013.01.011

30. Mahler R, Adler M. Type 2 Diabetes Mellitus: Update on Diagnosis, Pathophysiology, and Treatment. The Journal of Clinical Endocrinology & Metabolism. 1999;84(4):1165-1171. doi:10.1210/jcem.84.4.5612

31. Type 2 Diabetes: An Overview. TheDiabetesCouncil.com. https://www.thediabetescouncil.com/type-2-diabetes-an-overview/.

32. Type 2 Diabetes | NIDDK. National Institute of Diabetes and Digestive and Kidney Diseases. https://www.niddk.nih.gov/health-information/diabetes/overview/what-is-diabetes/type-2-diabetes.

33. Type 2 diabetes. Genetics Home Reference. https://ghr.nlm.nih.gov/condition/type-2-diabetes.

34. Gilmartin AB, Ural SH, Repke JT. Gestational diabetes mellitus. Rev Obstet Gynecol. 2008;1(3):129–134.

35. Gale E, Holleman F. Other types of diabetes mellitus - Diapedia, The Living Textbook of Diabetes. Diapedia.org. https://www.diapedia.org/other-types-of-diabetes-mellitus/4104085115.

36. Chen R, Ovbiagele B, Feng W. Diabetes and Stroke: Epidemiology, Pathophysiology, Pharmaceuticals and Outcomes. Am J Med Sci. 2016;351(4):380-386. doi:10.1016/j.amjms.2016.01.011

37. Seunggu Han M. Diabetes and stroke: The link, risk factors, and prevention. Medical News Today. https://www.medicalnewstoday.com/articles/324924.php.

38. Pitsavos C, Tampourlou M, Panagiotakos D et al. Association Between Low-Grade Systemic Inflammation and Type 2 Diabetes Mellitus Among Men and Women from the ATTICA Study. The Review of Diabetic Studies. 2007;4(2):98-104. doi:10.1900/rds.2007.4.98

39. Asahara T, Murohara T, Sullivan A et al. Isolation of Putative Progenitor Endothelial Cells for Angiogenesis. Science. 1997;275(5302):964-966. doi:10.1126/science.275.5302.964

40. George A, Bangalore-Prakash P, Rajoria S et al. Endothelial progenitor cell biology in disease and tissue regeneration. J Hematol Oncol. 2011;4(1):24. doi:10.1186/1756-8722-4-24

41. Hristov M, Weber C. Endothelial progenitor cells: characterization, pathophysiology, and possible clinical relevance. J Cell Mol Med. 2004;8(4):498-508. doi:10.1111/j.1582-4934.2004.tb00474.x

42. Urbich C, Dimmeler S. Endothelial Progenitor Cells. Circ Res. 2004;95(4):343-353. doi:10.1161/01.res.0000137877.89448.78

43. Liao S, Luo C, Cao B et al. Endothelial Progenitor Cells for Ischemic Stroke: Update on Basic Research and Application. Stem Cells Int. 2017;2017:1-12. doi:10.1155/2017/2193432

44. Yellon D, Davidson S. Exosomes. Circ Res. 2014;114(2):325-332. doi:10.1161/circresaha.113.300636

45. Edgar J. Q&A: What are exosomes, exactly?. BMC Biol. 2016;14(1). doi:10.1186/s12915-016-0268-z

46. Exosome Explosion. The Scientist Magazine®. https://www.the-scientist.com/features/exosome-explosion-42253.

47. Raposo G, Stoorvogel W. Extracellular vesicles: Exosomes, microvesicles, and friends. J Cell Biol. 2013;200(4):373-383. doi:10.1083/jcb.201211138

48. Crenshaw B, Gu L, Sims B, Matthews Q. Exosome Biogenesis and Biological Function in Response to Viral Infections. Open Virol J. 2018;12(1):134-148. doi:10.2174/1874357901812010134

49. Hu G, Drescher K, Chen X. Exosomal miRNAs: Biological Properties and Therapeutic Potential. Front Genet. 2012;3. doi:10.3389/fgene.2012.00056

50. Zha Q, Yao Y, Ren Z, Li X, Tang J. Extracellular vesicles: An overview of biogenesis, function, and role in breast cancer. Tumor Biology. 2017;39(2):101042831769118. doi:10.1177/1010428317691182

51. Yakimchuk K. Exosomes: isolation methods and specific markers. 2015;5. doi:10.13070/mm.en.5.1450

52. Exosomes 101 - Exosome Detection & Characterization | System Biosciences. System Biosciences. https://www.systembio.com/blog/exosomes-101-exosome-detection-characterization/.

53. Al Ahmad M. Electrical Detection, Identification, and Quantification of Exosomes. IEEE Access. 2018;6:22817-22826. doi:10.1109/access.2018.2828038

54. QIN J, XU Q. FUNCTIONS AND APPLICATIONS OF EXOSOMES. Acta Poloniae Pharmaceutica-Drug Research. 2014;71(4):537-543. http://ptfarm.pl/pub/File/Acta_Poloniae/2014/4/537.pdf.

55. Biological functions, isolation and detection strategies for exosomes. Exosome-rna.com. https://www.exosome-rna.com/biological-functions-isolation-and-detection-strategies-for-exosomes/. 2017.

56. Li X, Chen C, Wei L et al. Exosomes derived from endothelial progenitor cells attenuate vascular repair and accelerate reendothelialization by enhancing endothelial function. Cytotherapy. 2016;18(2):253-262. doi:10.1016/j.jcyt.2015.11.009

57. Li X, Jiang C, Zhao J. Human endothelial progenitor cells-derived exosomes accelerate cutaneous wound healing in diabetic rats by promoting endothelial function. J Diabetes Complicat. 2016;30(6):986-992. doi:10.1016/j.jdiacomp.2016.05.009

58. Zhang J, Chen C, Hu B et al. Exosomes Derived from Human Endothelial Progenitor Cells Accelerate Cutaneous Wound Healing by Promoting Angiogenesis Through Erk1/2 Signaling. Int J Biol Sci. 2016;12(12):1472-1487. doi:10.7150/ijbs.15514

59. Ke X, Yang D, Liang J et al. Human Endothelial Progenitor Cell-Derived Exosomes Increase Proliferation and Angiogenesis in Cardiac Fibroblasts by Promoting the Mesenchymal–Endothelial Transition and Reducing High Mobility Group Box 1 Protein B1 Expression. DNA Cell Biol. 2017;36(11):1018-1028. doi:10.1089/dna.2017.3836

60. Jia Y, Zhu Y, Qiu S, Xu J, Chai Y. Exosomes secreted by endothelial progenitor cells accelerate bone regeneration during distraction osteogenesis by stimulating angiogenesis. Stem Cell Res Ther. 2019;10(1):12. Published 2019 Jan 11. doi:10.1186/s13287-018-1115-7

61. Wang S, Aurora A, Johnson B et al. The Endothelial-Specific MicroRNA miR-126 Governs Vascular Integrity and Angiogenesis. Dev Cell. 2008;15(2):261-271. doi:10.1016/j.devcel.2008.07.002

62. Zhou Q, Anderson C, Hanus J et al. Strand and Cell Type-specific Function of microRNA-126 in Angiogenesis. Molecular Therapy. 2016;24(10):1823-1835. doi:10.1038/mt.2016.108

63. Qu M, Pan J, Shi X, Zhang Z, Tang Y, Yang G. MicroRNA-126 is a prospective target for vascular disease. Neuroimmunol Neuroinflamm. 2018;5(4):10. doi:10.20517/2347-8659.2018.01

64. Pan Q, Zheng J, Du D et al. MicroRNA-126 Priming Enhances Functions of Endothelial Progenitor Cells under Physiological and Hypoxic Conditions and Their Therapeutic Efficacy in Cerebral Ischemic Damage. Stem Cells Int. 2018;2018:1-13. doi:10.1155/2018/2912347

65. LIU Y, ZHOU Y, FENG X et al. MicroRNA-126 functions as a tumor suppressor in colorectal cancer cells by targeting CXCR4 via the AKT and ERK1/2 signaling pathways. Int J Oncol. 2013;44(1):203-210. doi:10.3892/ijo.2013.2168

66. Suresh Babu S, Thandavarayan R, Joladarashi D et al. MicroRNA-126 overexpression rescues diabetes-induced impairment in efferocytosis of apoptotic cardiomyocytes. Sci Rep. 2016;6(1). doi:10.1038/srep36207

67. Mulcahy L, Pink R, Carter D. Routes and mechanisms of extracellular vesicle uptake. J Extracell Vesicles. 2014;3(1):24641. doi:10.3402/jev.v3.24641

68. Wang J, Chen S, Ma X et al. Effects of Endothelial Progenitor Cell-Derived Microvesicles on Hypoxia/Reoxygenation-Induced Endothelial Dysfunction and Apoptosis. Oxid Med Cell Longev. 2013;2013:1-9. doi:10.1155/2013/572729

69. Li P, Kaslan M, Lee S, Yao J, Gao Z. Progress in Exosome Isolation Techniques. Theranostics. 2017;7(3):789-804. doi:10.7150/thno.1813